

**Zeitschrift:** IABSE reports = Rapports AIPC = IVBH Berichte  
**Band:** 999 (1997)

**Rubrik:** Fire resistance

#### **Nutzungsbedingungen**

Die ETH-Bibliothek ist die Anbieterin der digitalisierten Zeitschriften auf E-Periodica. Sie besitzt keine Urheberrechte an den Zeitschriften und ist nicht verantwortlich für deren Inhalte. Die Rechte liegen in der Regel bei den Herausgebern beziehungsweise den externen Rechteinhabern. Das Veröffentlichen von Bildern in Print- und Online-Publikationen sowie auf Social Media-Kanälen oder Webseiten ist nur mit vorheriger Genehmigung der Rechteinhaber erlaubt. [Mehr erfahren](#)

#### **Conditions d'utilisation**

L'ETH Library est le fournisseur des revues numérisées. Elle ne détient aucun droit d'auteur sur les revues et n'est pas responsable de leur contenu. En règle générale, les droits sont détenus par les éditeurs ou les détenteurs de droits externes. La reproduction d'images dans des publications imprimées ou en ligne ainsi que sur des canaux de médias sociaux ou des sites web n'est autorisée qu'avec l'accord préalable des détenteurs des droits. [En savoir plus](#)

#### **Terms of use**

The ETH Library is the provider of the digitised journals. It does not own any copyrights to the journals and is not responsible for their content. The rights usually lie with the publishers or the external rights holders. Publishing images in print and online publications, as well as on social media channels or websites, is only permitted with the prior consent of the rights holders. [Find out more](#)

**Download PDF:** 16.01.2026

**ETH-Bibliothek Zürich, E-Periodica, <https://www.e-periodica.ch>**

## Bridging and Restraint Effects of Localised Fires in Composite Frame Structures

**Colin BAILEY**

Senior Engineer  
The Steel Construction Inst.  
Ascot, UK

**Ian BURGESS**

Senior Lecturer  
University of Sheffield  
Sheffield, UK

**Roger PLANK**

Professor  
University of Sheffield  
Sheffield, UK

### Summary

Software developed at the University of Sheffield was used to model one of a series of fire tests on the full-scale composite test frame at Cardington, in which a single beam was heated. The effect of local buckling, which occurred in the test, on the beam's overall behaviour was investigated using the software. Both analyses and test showed that the cool adjacent structure has a beneficial effect on the behaviour of the heated beam, permitting redistribution of load by bridging to the adjacent structure. This is seen to diminish as the fire compartment is increased to a more realistic size.

### 1. Introduction

Structural fire engineering is a relatively new philosophical approach to the design of structures against collapse in a fire. For steel structures recent limit state fire engineering design codes include BS5950 Part 8<sup>1</sup> and EC3 Part 1.2<sup>2</sup>, as well as EC4 part 1.2<sup>3</sup> which covers the fire resistant design of composite structures. These codes, which classify fire as an accidental limit state, are based on load levels which are statistically likely during a fire, material stress-strain relationships at elevated temperatures and non-uniform heating where applicable. This concept, which provides a new range of fire resistance options, is slowly beginning to replace the traditional approach of retrospectively prescribing a thickness of protective coating to steelwork.

In the UK it has recently been estimated that fire protection contributes 23% of the overall cost of typical commercial frames. Also, the hidden costs involved in actually fixing the protection and consequent programme delays need to be considered. The use of fire engineering principles can result in considerable cost savings compared with the traditional approach, since standard protection thicknesses are specified from manufacturers' tables which are implicitly based on limiting the maximum temperature of the steel to 550°C. This is the temperature at which, in simplistic terms, it has been assumed that the yield strength of steel is reduced to the extent that an ultimate strength design loses its safety margin. However, this assumption is based on the steel being uniformly heated and fully stressed at ambient temperature, and also ignores the fact that stress-strain curves become highly non-linear at elevated temperatures.

Although the new design codes have provided a more scientific approach to assessing the response of steel-framed buildings in fire they are limited by being based on isolated member design, developed from standard furnace tests. The failure criteria for isolated members in standard fire tests are defined in terms of displacement, and are set at values which prevent damage to the furnace during testing. However, the validity of basing full-structure predictions on the behaviour of isolated members is highly questionable, and recent research has increasingly been focused on

the full structural behaviour of buildings in fire. In the UK this has included a series of fire tests conducted during 1995 and 1996 on a full-scale composite test frame, constructed by the Building Research Establishment at its Cardington Laboratory. The main aim of the tests was to provide extensive experimental data as a validation for computer software which can predict the structural response of the building during a fire.

Because of the very high cost and limited validity of fire tests, reliable computer software is required to allow different structural and fire scenarios to be studied economically. At the University of Sheffield a purpose-written computer program<sup>4</sup> has been developed which can sensibly be used on a standard Personal Computer. Previous predictive model analyses using this software, as well as observations from the tests, have shown that the surrounding cold structure, in particular the continuous flooring system, has a significant beneficial effect on the behaviour of the heated zone. However, the area of the heated zone in these cases has been very limited, and it is predictable that the support provided by the surrounding structure might diminish in a more realistic scenario in which the fire compartment is more extensive. To investigate the effect of increasing the fire compartment size the model was validated against the first fire test on the Cardington frame, and then the compartment size increased to a more realistic size.

The computer software is capable of predicting the structural response of steel-framed buildings subject to any specified fire scenario. The steel beam-column members are represented by two-noded one-dimensional finite elements which are capable of modelling three-dimensional response including warping, and incorporate a high degree of both material and geometrical nonlinearity at ambient and elevated temperatures. Arbitrary temperature distributions can be specified through the cross-section and also along the length of a steel member. Semi-rigid connection behaviour can be modelled using spring elements with any specified moment-rotation-temperature relationship. The floor slab is represented by four-noded shell elements which can be connected to the one-dimensional beam elements at a common nodal point, thus modelling full composite action between the steel framing and the supported floor. Thermal strains due to heating the concrete are also included. An extremely simple cracking model has been used to represent the behaviour of the concrete floor based on limiting the bending stress in the shell elements.

## 2. Comparison with a Cardington Fire Test

On 19 January 1995, the first of a series of fire tests was carried out by British Steel. The test building consisted of an eight-storey steel frame acting compositely with the supported floor slabs via shear studs. The building footprint was 21m x 45m, with the general structural layout shown in Fig. 1. The floor was of typical UK composite construction, consisting of 0.9mm thick steel deck (PMF CF70) with lightweight concrete and A142 anti-crack mesh. The overall specified depth of the slab was 130mm. The fire test involved heating a secondary beam on the 7th floor, over the central 8.0m of its 9.0m length, as shown in Fig. 1.

Previous computer simulations<sup>5</sup> have been conducted of this test, in which the beam was modelled as an isolated composite section (Fig. 2) and as a sub-frame which included a large area of cold structure including the continuous floor slab, as shown in Fig. 1. The comparison between the test results and computer simulations is shown in Fig. 2, with the local deflected shape shown in Fig. 3 at a steel beam flange temperature close to the maximum measured during the test.

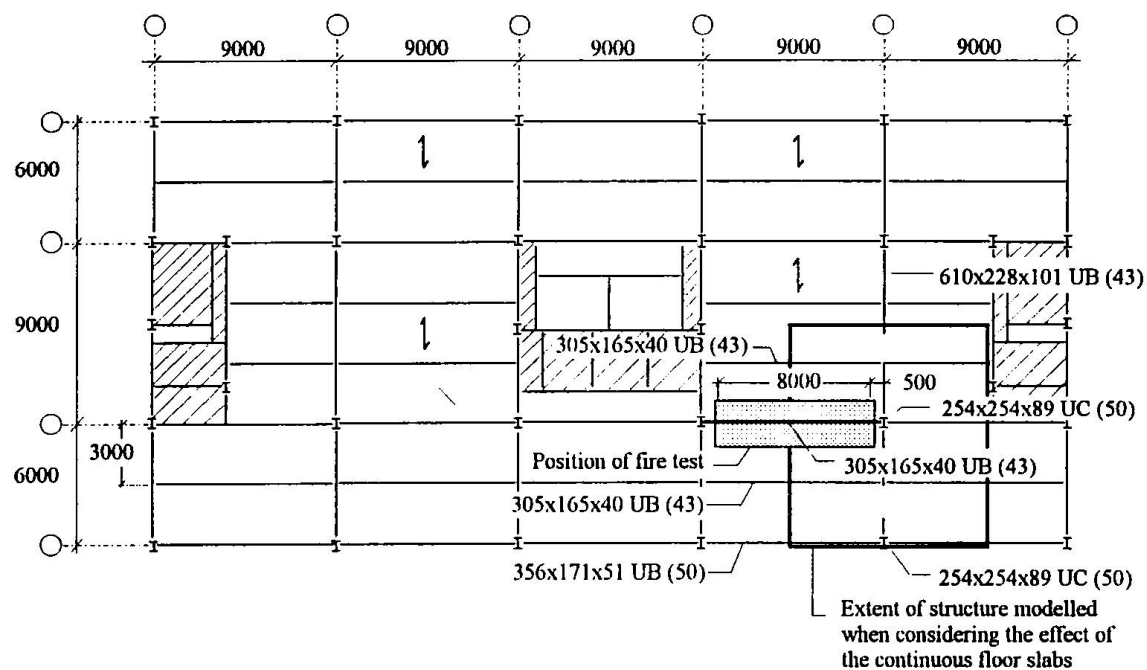


Fig. 1 General layout of test frame and position of first fire test.

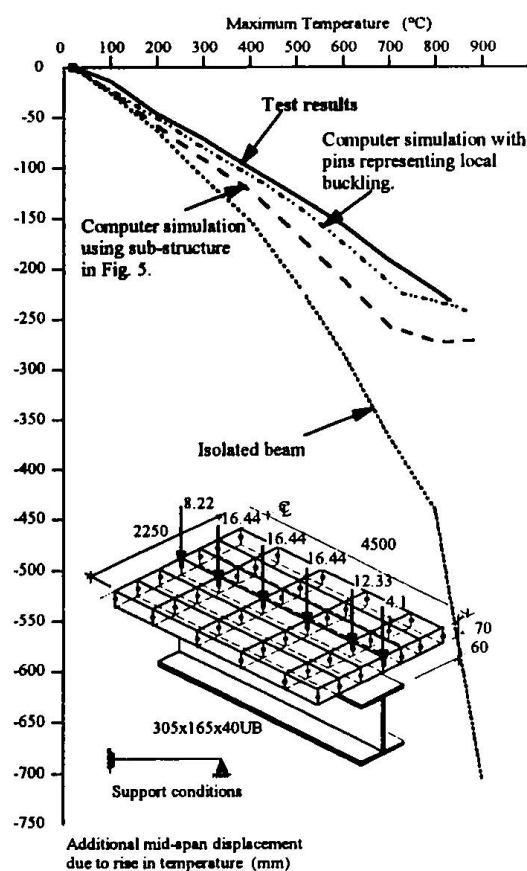


Fig. 2 Comparison between computer predictions and test results.

Inclusion of the behaviour of the continuous floor slab in the computer simulation clearly has a significant influence on the behaviour, compared to the equivalent isolated beam. Comparison with the test results shows that using the sub-frame model reasonable predictions are obtained, showing clearly the beneficial effect of the "bridging" action by the slab across the heated beam, an action which transfers load to the surrounding cold structure. This form of load transfer away from the heated member could not be achieved without the continuity in the slab which is inherent in this form of composite construction.

On removal of the furnace following the test it was found that local buckling had taken place in the exposed flange of the steel beam at a position just inside the furnace. It can be surmised that this was caused by the high axial forces due to restraint of thermal expansion, together with the negative moment occurring at this position during the rise in temperature. This type of buckling had previously been seen during the investigation following the Broadgate Fire<sup>6</sup> in the UK. Since one-dimensional finite elements are used to represent the steel members local distortional buckling cannot be modelled. However, to investigate the influence of

local buckling the previous computer simulation was re-run with spring elements of zero rotational rigidity inserted at the positions of local buckling. Due to numerical problems removal of axial stiffness in the buckled areas was not possible, although this was not considered to be significant since in composite construction of this type the axial force would in practice be redirected through the slab. Inserting these pins from the start of the computer simulation of the test is over-conservative, but nevertheless it provides an indication of the significance of local buckling. The predictions from this simulation are shown in Fig. 2, in which it can be seen that the local buckling does not have a major effect on the behaviour of the beam, but causes slightly lower displacements. The reason for lower predicted displacements is mainly due to the failure of the concrete in the hogging zones. This can be explained by considering a fixed-ended beam for which the position of the points of contraflexure is at 0.21 of the beam span from its ends. If this is compared with the present case where the position of the points of contraflexure is set at the local buckling position, 0.06 of the span from its ends, it can be seen that less of the beam's length is in hogging, resulting in less concrete cracking and thus a stiffer beam.

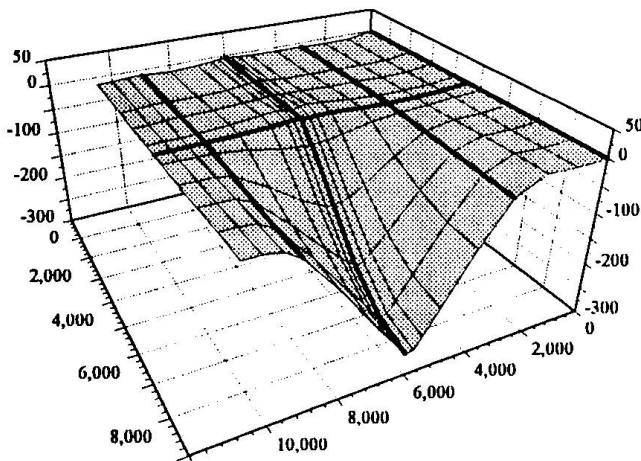


Fig. 3 Deflections of the local area at 800°C.

Inserting a pin at each position of local buckling is conservative, since it assumes that local buckling is present from the start of the test whereas in reality it would occur at a reasonably late stage during heating. Therefore the two curves representing the behaviour with and without pins can be classed as upper and lower bounds, with the actual behaviour changing from the one to the other as heating progresses.

Intuitively it might be expected that local buckling in the steel beam, caused by the restraint of the surrounding structure, would be detrimental to the fire resistance of the beam, rather than

beneficial as is shown in the simulation. However, the position at which local buckling occurred in this particular test was governed by the location of the furnace. In a naturally occurring fire the whole beam would normally be affected, with the ends possibly being slightly cooler. Therefore it would be expected that if local buckling did occur then it would be at positions very close to the connections, as observed in the aftermath of the Broadgate Fire. This can be viewed as the beam transforming from a semi-rigid to a simply supported member, resulting in larger displacements. In order to simulate local buckling in detail the beam cross-section would need to be modelled using shell elements rather than the existing line elements. This would increase the computer runtime very considerably, probably reduce the area of structure which can practically be modelled and almost certainly result in a need to transfer the analysis away from the PC platform. Alternatively a conservative approach might be to treat all steel-to-steel connections as pinned, to allow for any possible detrimental effect that could occur due to local buckling.

### 3. Extension of the Fire-Affected Area

Both the fire test and computer simulations have shown clearly the beneficial effect of bridging action and the detrimental effect of local buckling in composite-framed buildings. However the

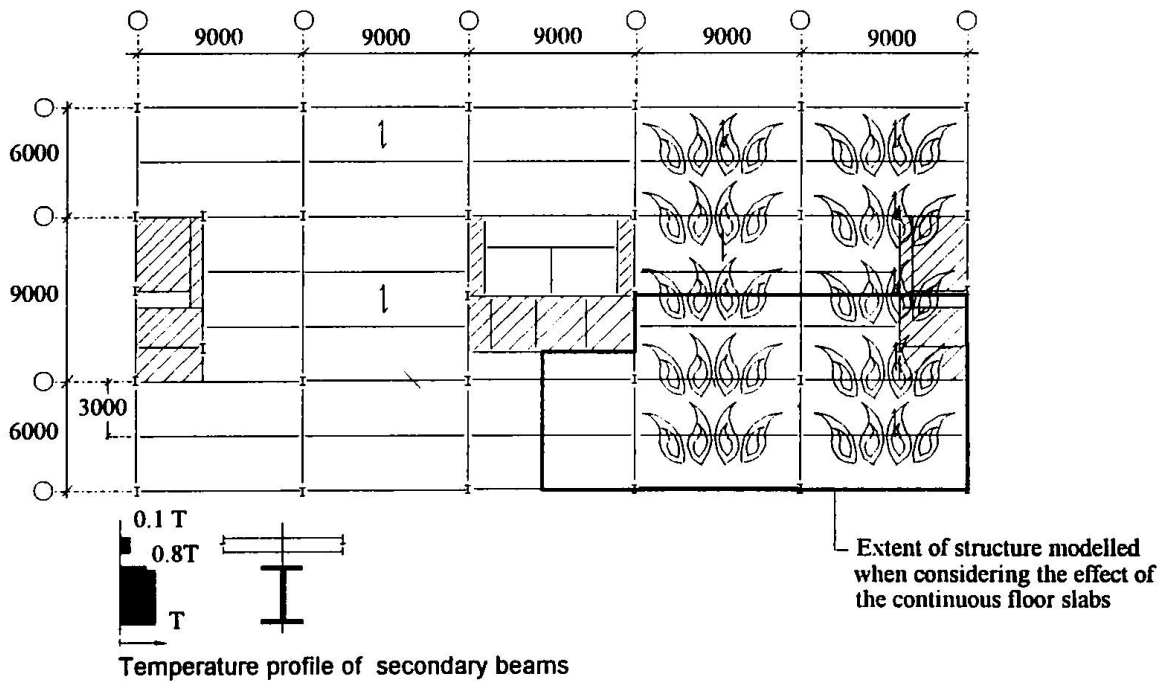


Fig. 4 Large compartment fire.

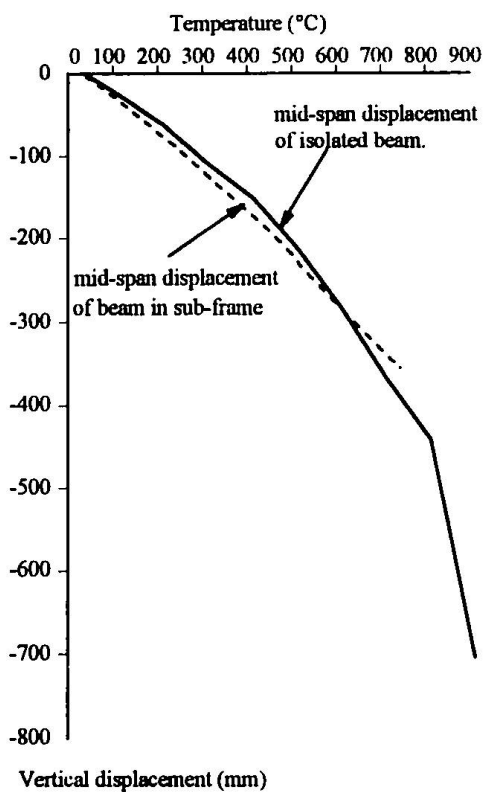


Fig. 5 Computer predictions.

fire-affected area in this test was very small, and in a more usual scenario the fire might affect much more of the structure. This will depend on compartment size and on the compartment walls maintaining their integrity during a fire. The size of a compartment depends largely on the building's use. At one extreme are hotels, nursing homes, etc., where compartments are defined by room sizes, and at the other airports, sports halls, etc, where compartments tend to be defined by the extent of the building plan.

A simulation was performed with the extent of the fire-affected structure increased as shown in Fig. 4, to cover a more realistic area in an office building. All beams were heated at the same rate. The columns were protected and therefore considered to retain their full strength in the analysis. To represent local buckling, all steel-to-steel connections were represented as pinned. The mid-span displacements of the beam from the previous example are shown in Fig 5 for this case. It can be seen that the beam's behaviour is now very close to the prediction for an isolated member, indicating that little beneficial effect is now being obtained from bridging action across the floor slabs. The deflected shape of the slabs and beams in the affected zone at 730°C is shown in Fig. 6.

#### 4. Conclusions

A finite element code capable of predicting the structural response of steel-framed buildings has been developed at the University of Sheffield. This program has shown to give very good predictions of the fire tests conducted on the full scale composite test frame at Cardington. Since one-dimensional finite elements are used to represent the steel members, local buckling, which was found to occur in the first fire test, cannot be predicted. Nevertheless, to investigate the influence of local buckling spring elements were used to represent a pinned connection at the positions of local buckling in the test. Since in reality local buckling occurred at a certain temperature during the test, the insertion of pins from the start of the computer simulation is very conservative.

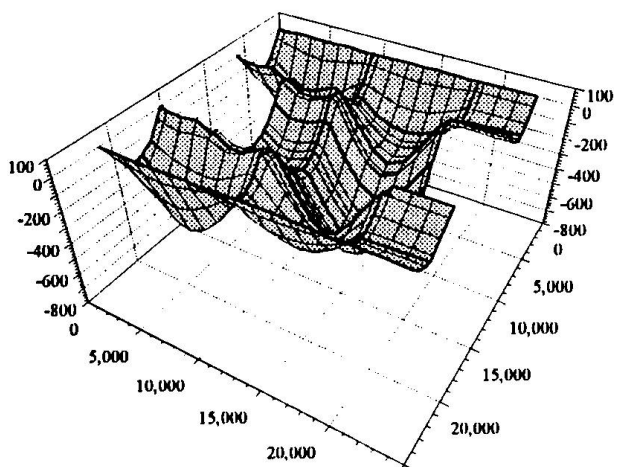


Fig. 6. Deflection of large compartment at 730°C.

The results showed that local buckling had little effect on the heated beam's behaviour and in fact the computer simulation indicated that local buckling resulted in lower displacements. This was attributed to the position of the local buckling, determined by the size of the furnace, which influenced the extent of concrete failure. In normal circumstances, if local buckling of beams did occur in a fire it would be in the vicinity of the connections. This would effectively transform the semi-rigid connections to simple connections which would be detrimental to the fire resistance.

It is clear that fire-affected zones of structure can use the adjacent cool structure for re-direction of the local loading paths (the action referred to as bridging), which is advantageous from the viewpoint of fire resistance. However, as the size of the fire compartment increases the support from these areas, as well as their restraint to thermal expansion, diminishes so that the behaviour more closely resembles that of isolated members in furnace testing.

#### References

1. BS5950: 1985, *Structural use of steelwork in building. Part 8: Code of Practice for Fire Resistant Design*, BSI, London, 1988.
2. Eurocode 3, *Design of steel structures. Part 1.2: Structural Fire Design (Draft)*, Commission of the European Communities, 1990.
3. Eurocode 4, *Design of composite steel and concrete structures. Part 1.2: Structural Fire Design (Draft)*, Commission of the European Communities, 1992.
4. Bailey C.G., Simulation of the structural behaviour of steel-framed buildings in fire. Ph.D. Thesis, University of Sheffield, UK, 1995.
5. Bailey, C.G., Burgess, I.W., & Plank, R.J., "Computer simulation of a full-scale structural fire test". *Structural Engineer*, 74 (6) (1996) 93-100.
6. *Structural Fire Engineering. Investigation of Broadgate Phase 8 Fire*. The Steel Construction Institute, Ascot, UK, 1991.

## Compression Membrane Action in Composite Slabs

**R.J. PEEL CROSS**

Ernest Griffiths and Son  
Liverpool, UK

**G.I.B. RANKIN**

Dr  
Queen's University  
Belfast, UK

**S.G. GILBERT**

Dr  
Queen's University  
Belfast, UK

**A.E. LONG**

Professor  
Queen's University  
Belfast, UK

### Summary

This paper discusses the results from a two year research project which studied the effects of Compressive Membrane Action (CMA) on composite metal decking/concrete slabs before and after fire. The paper concentrates on work carried out on full scale slabs in the BRE test building at Cardington, but compares these results with those obtained from slab strips tested in the laboratory. It was found that fire damaged slabs exhibited far greater strengths than previously supposed, some held loads higher than those predicted by yield line analysis.

### 1. Introduction

Compressive Membrane Action is the two way arching effect which occurs when a laterally restrained slab is loaded (1). The load is resisted by a compressive force which extends through the slab from the load to the supports (see Fig 1). The greater the element depth/length ratio is, the greater is the amount of arching which occurs. CMA is already used to justify a reduction in the amount of reinforcing steel used in certain beam and slab bridge decks (2), but has not yet been applied in practice to other structures (3). The purpose of this research was to find out whether CMA contributes to the strength of composite metal decking/concrete slabs in buildings, and whether it helps to sustain load in a composite slab which has been badly damaged by fire (4).

Thus, a series of full scale in-situ and laboratory tests was devised to investigate the effects of the following parameters:

- a) slab boundary conditions - interior, edge and corner composite slabs were tested and
- b) fire damage - composite slabs were tested before and after fire loading.

### 2. Tests at BRE Cardington

The full scale in-situ tests were carried out in the Building Research Establishment's 'Large Building Test Facility' (LBTF) at Cardington, UK. The building is eight storeys high and replicates a typical steel framed, composite slab office block with a design dead load of

3.65kN/m<sup>2</sup> and design imposed load of 3.5kN/m<sup>2</sup>. It has been built purely for research purposes, in particular to assess the effect of fire on a 'real' building.

The tests were carried out in two phases, the first on undamaged slabs (pre-fire tests) and the second on fire damaged slabs (post-fire tests) at the locations indicated in Fig 2. Each set of slabs underwent two tests, the first being a proof load test and the second an ultimate load test. Loads were applied along the quarterpoints of the slab in order to simulate the bending moments due to a uniformly distributed load. The load was applied hydraulically using ten 30 tonne jacks (Fig 3), except for the service load on the fire damaged slabs which was applied incrementally with 1.1 tonne sandbags. This was mainly because the panels were so distorted by the fire that it would have been difficult to line up holes for the Macalloy bars over two floors. In addition, it was known that the slabs had sustained a superimposed load of about 2.4kN/m<sup>2</sup> during the fire test and it was decided not to load the slab more than this in case the beam connections failed.

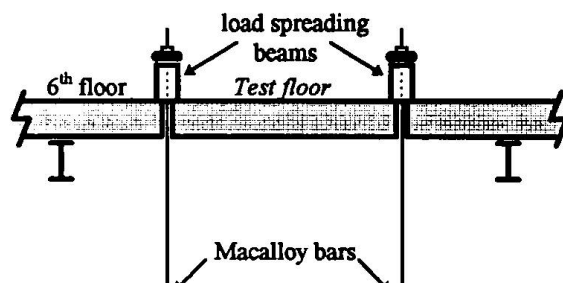
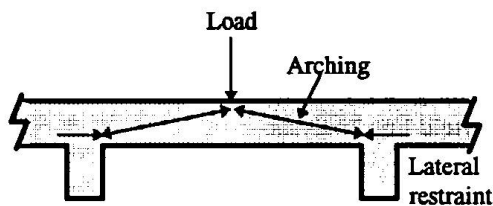


Fig.1 Arching action

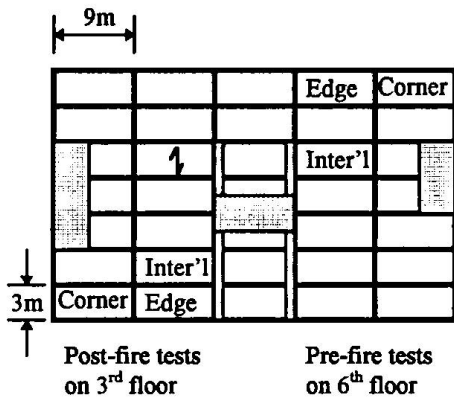


Fig.2 Cardington test panels

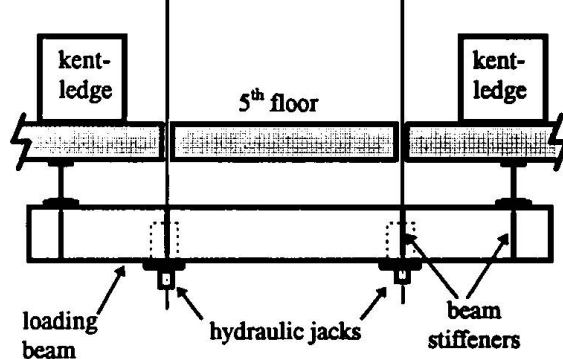


Fig.3 Hydraulic floor loading system

## 2.1 Proof load tests

### 2.1.1 Pre-fire proof load tests

The slabs were first loaded in 1.2kN/m<sup>2</sup> increments up to an applied test load of 5.6kN/m<sup>2</sup> (1.25 Dead load + 1.25 Imposed load - slab self-weight - weight of test apparatus). Deflections were measured at each increment of load with a staff and level. This test was carried out twice and then the load was allowed to remain on the slab for 24 hours. The deflections were taken before and after to ascertain whether any significant creep had occurred. The slabs deflected less than

1/400 of the 3m span under the imposed load, and the 24 hour tests showed that no creep occurred.

### 2.1.2 Post-fire proof load tests

Before these tests began, the slabs were subjected to a fire load of up to  $763^{\circ}\text{C}$ . This procedure is described in more detail in the BRE's newsletter, LBTF News, Issue 13, Summer 1996. For this test it was decided to only load the slabs once as the floor was fairly badly damaged, and moving the sandbags on and off the floor was causing the cracks along the edge of the slab to open up further. The load was taken up to a superimposed UDL of  $2.4\text{kN/m}^2$ . Although this load was less than half the load for the pre-fire tests, the deflections were fairly similar, indicating that the slab was not maintaining load as well as before the fire. However this was to be expected, as the steel frame had badly deformed, making the whole structure much less rigid.

Slab location	Pre-fire tests: Deflection under $5.6\text{kN/m}^2$ imposed load (mm)	Post-fire tests: Deflection under $2.4\text{kN/m}^2$ imposed load (mm)
Internal	7	6
Edge	4.5	4
Corner	Test not carried out	5

Table 1 Comparison of slab central deflections before and after fire

## 2.2 Ultimate load tests

The test rig set up was slightly different from the proof load tests (Fig 3), because only the slab was to be loaded to failure. As it was imperative that the steel frame did not fail, the test rig was moved up one floor so that it was immediately under the slab being tested. This created a self-straining system whereby the load on the slab was resisted by the reactions of the loading rig against the steel beams.

### 2.2.1 Pre-fire ultimate load tests

The slabs were loaded in  $1.2\text{kN/m}^2$  intervals, until they approached failure when the loading increments were reduced to  $0.6\text{kN/m}^2$ . At a load of about  $15\text{kN/m}^2$ , the decking began to debond noisily from the concrete. It is likely that this was the point at which the concrete began to crack as well, but this was impossible to see with the decking in place. At this point, the stiffness of the slab reduced by about 60%. At about 2/3 of the ultimate load level, yielding of the decking began to occur and the rate of deflection progressively increased until failure.

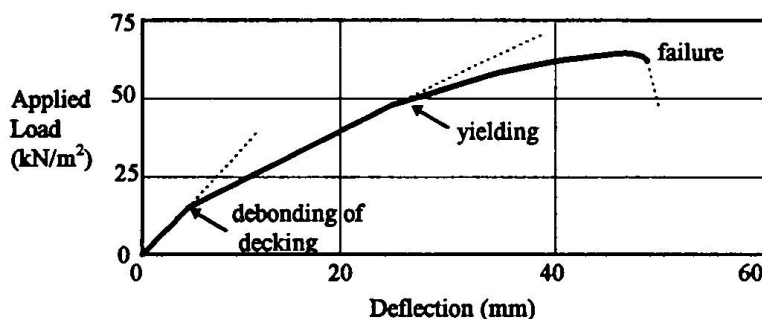


Fig. 4 Pre-Fire Load/Deflection Results for Internal Panel

In all cases, failure consisted of a sudden, shear failure along one of the edges parallel to the spanning direction of the slab. The failure loads are shown in Table 2. It can be seen that the strengths of the panels (except the post-fire internal panel) were considerably greater than the predicted yield line loads, particularly for the pre-fire internal panel.

In general, the failure load was related to the depth of the slab, which varied across the floor. However, the internal panel sustained a significantly higher load than the edge and corner slabs, even though it was the least deep. This implies that the internal slab was restrained to a greater extent by the surrounding slabs and beams indicating that there was a greater contribution of CMA to the load carrying capacity of the internal slab.

#### 2.2.2 Post-fire ultimate load tests

The fire load caused the slabs to crack along the beam lines. The slabs had deflected with the steel beams which had deformed greatly due to the fire load. In these tests the decking was not heard to debond - presumably because this had already occurred under the fire load. As failure was approached, the load was carefully controlled so that the slabs did not fail catastrophically.

A summary of the failure loads is given in Table 2. The edge and corner slabs were not as badly damaged as the internal panel in the fire and their failure loads were correspondingly higher. The internal panel had deflected by nearly half a metre in places and so was much less rigid than in the pre-fire tests. It is interesting to note that, even after the fire, all the panels withstood at least three times the required design ultimate load of  $10.7\text{kN/m}^2$ .

Slab location	Cardington failure load - $P_{CAR}$ ( $\text{kN/m}^2$ )	Yield line load - $P_{YL}$ ( $\text{kN/m}^2$ )	$P_{CAR}/P_{YL}$
<b>Pre-fire</b>			
Internal	69.9	37.4	1.87
Edge	61.4	39.2	1.57
Corner	62.4	41.9	1.49
<b>Post-fire</b>			
Internal	38.0 (54%)*	38.9	0.98
Edge	46.4 (75%)*	38.5	1.20
Corner	47.4 (76%)*	37.0	1.28

\* % of pre-fire failure load

Table 2 Cardington Test Results and Theoretical Failure Loads

### 3. Laboratory Tests at Queen's University, Belfast

Four tests were carried out to assess the effect of fire on a slab. Two of the slabs were simply supported and two were laterally restrained using a rig that had been built for the purpose. The specimens were designed to be similar to the slabs at Cardington, so were made 3000 mm long and 130 mm deep. Comflor CF70 metal decking was used, as at Cardington, and a typical decking profile is shown in Fig 5. Debonding of the decking due to fire damage was simulated by greasing the decking with a release agent before casting the slab. The results of the tests are shown in Table 3.

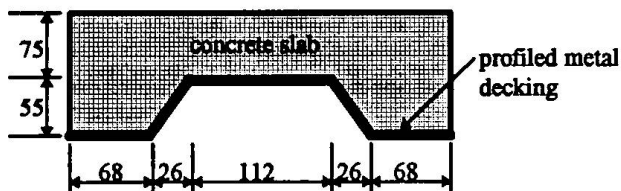


Fig. 5 Cross-section of composite slab strip

The slabs were loaded incrementally to failure using a Dartec electro-hydraulic actuator, and readings of load and central deflection were taken at each increase in load. For the pre-fire tests the decking could be heard debonding from the slab at a load of about  $14.4\text{kN/m}^2$  which is similar to the level of load at which this occurred in Cardington. The post-fire simulations showed that the slab still had considerable strength, even though the decking was not bonded to the slab. This agreed with the full panel results from Cardington.

Slab type	Failure load ( $\text{kN/m}^2$ )
<b>Pre-fire tests (with decking)</b>	
Simply supported	34.3
Restrained	65.9
<b>Post-fire tests (debonded decking)</b>	
Simply supported	27.9
Restrained	34.5

Table 3 Laboratory Test Results

#### 4. Comparison of Results

The Cardington test results are compared with the laboratory test results in Table 4. The failure loads for the Cardington slabs are first compared with the failure loads for the simply supported laboratory strips. The ratios of  $P_{CAR}/P_{LAB(SS)}$  show that the strength of real panels tested in-situ was considerably greater than the conventional simply supported design strength. This strength enhancement is mainly attributable to the presence of rotational and lateral restraint at the slab boundaries which gives rise to boundary moments and Compressive Membrane Action. As the internal panel had the greatest degree of restraint it exhibited the greatest strength enhancement (except in the post-fire test where the internal panel was the most severely damaged by the fire).

The ratios of  $P_{CAR}/P_{LAB(RES)}$  for the pre-fire tests show that the high degree of restraint used in the laboratory was close to that of the internal panel at Cardington but was greater than that for the edge and corner panels. The post-fire test results again reflect the more severe damage to the Cardington internal panel than the edge and corner panels and also indicate that the edge and corner panels had greater residual strength than the laboratory results suggested.

All of the slabs exhibited strengths far greater than the ultimate design load of  $10.7\text{kN/m}^2$ ,

which shows that even after a fire, although the slab would be unserviceable, it may be possible to rely on the residual strength of the slab for safety purposes.

Slab type	$P_{CAR}/P_{LAB(SS)}$	$P_{CAR}/P_{LAB(RES)}$
<b>Pre-fire</b>		
Internal	2.04	1.06
Edge	1.79	0.93
Corner	1.82	0.95
<b>Post-fire</b>		
Internal	1.36	1.17
Edge	1.66	1.43
Corner	1.70	1.46

*Table 4 Comparison of Cardington and Laboratory Test Results*

## 5. Conclusions

- The strengths of the composite metal decking/concrete slab panels in the BRE Cardington test building were found to be significantly greater than the ultimate capacities predicted by yield line theory. This strength enhancement is mainly attributable to the effect of boundary conditions which induce boundary moments and Compressive Membrane Action.
- The load capacity of composite slabs that have been subjected to an intense fire is primarily reduced by debonding of the metal decking and a reduction in the CMA contribution due to deformation of the steel frame.
- Providing the connections in the steel frame of the building remain intact, fire damaged composite slabs can still sustain a load greater than the required design ultimate load, although greatly increased deformations of the steel frame may render these slabs unserviceable.

## 6. References

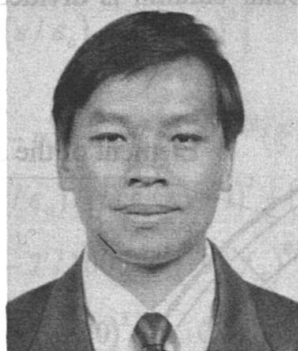
1. OCKLESTON A J (June 1958), 'Arching actions in reinforced concrete slabs', *The Structural Engineer*, Vol 36, No 6, pp 197-201.
2. KIRKPATRICK J, RANKIN G I B, LONG A E (1986), 'The influence of CMA on the serviceability of beam and slab bridge decks'. *The Structural Engineer*, Vol 64B, No 1, March, pp 6-9 & 12.
3. LONG A E, RANKIN G I B (1989), 'Real strength and robustness of reinforced concrete structures'. *Conservation of Engineering Structures*, Thomas Telford, London, pp 47-58.
4. PEEL CROSS R J (1996), 'Compressive Membrane Action in Composite Slabs'. MPhil thesis, Civil Engineering Department, Queen's University, Belfast, 101 pp.

## 7. Acknowledgements

The authors gratefully acknowledge the support provided by the EPSRC, BRE and Comflor Ltd.

## New Developments in Fire Resistance of Concrete Filled Steel Tubes in China

**Lin-Hai HAN**  
Civil Engineering Professor  
Harbin University  
Harbin, China



Lin-Hai Han, born 1967, did his PhD in Harbin University of Civil Engineering and Architecture in 1993, major in Structural Engineering.

### Summary

Finite element method is applied for the calculations of temperature fields of concrete filled steel tubes under fire. A theoretical model that calculates deformations and strength of column in fire and fire resistance is described in this paper. A comparison of results calculated using this model with the results of tests, there is good agreement. Based on the theoretical model, influence of the changing strength of the materials, diameter, steel ratio and slenderness ratio on the fire resistance is discussed.

### 1. Introduction

Concrete filled steel tubular columns have been used extensively in China as well as other countries, they have proved to be economical in themselves as well as leading to rapid construction and thus additional cost savings. An important criterion for the design of concrete filled steel tubes, besides the serviceability and critical load bearing capacity, is an adequate fire resistance.

Research to determine the fire resistance of concrete filled steel tubular column has been carried out in several countries in the world<sup>[1-7]</sup>. In recent years, Harbin University of Civil Engineering and Architectures (HUCEA) has been engaged in research to calculate the fire resistance of concrete filled steel tubular columns with the support of the Chinese Natural Science Foundation. Both theoretical and experimental studies were carried out<sup>[8,9]</sup>. Most of the HUCEA has been carried out on columns with circular cross-section, and the columns have been subjected to axial compression or eccentric compression loads.

The composite action between the steel and concrete has been considered, which was often neglected by other researchers in the theoretical analysis. A theoretical model that calculates the strength and the fire resistance of the columns is described in this paper, and influence of the changing parameters of the column on the fire resistance are analyzed.

## 2. Strength of Columns During Fire Exposure

### 2.1 Division of Cross-Section

To calculate the temperatures, deformations and stresses in the columns and its strength, the cross sectional area of the concrete filled steel tubular column is divided into a number of annular elements, show as in Figure 1.

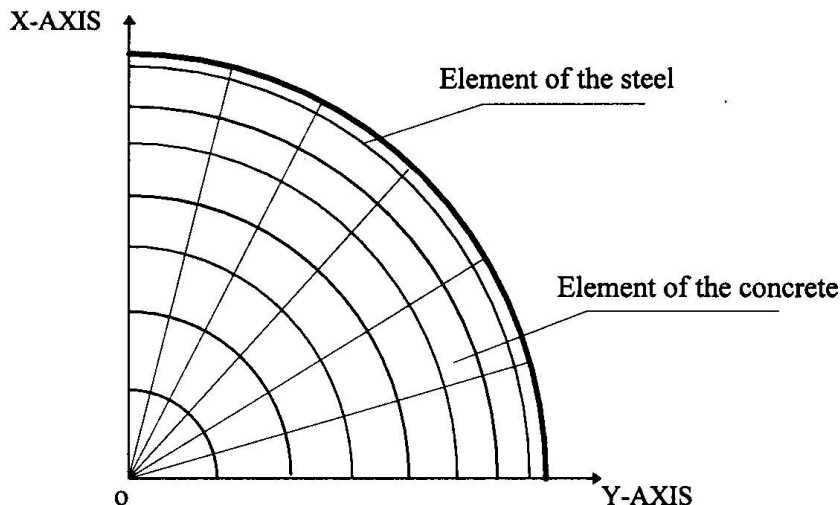


Figure 1 Arrangement of elements in quarter section

### 2.2 Temperature of Columns During Fire

The column temperatures are calculated by finite element method. The method for deriving the heat transfer equations and calculating temperatures, with the thermal properties is described in detail in Reference(8). The temperature of an element in Figure 1 is assumed to be equal to the temperature at its center.

### 2.3 Stress-Strain Relations of the Steel and Concrete

The basic reason that concrete filled steel tubular structures differ from tubular steel structures, is that there exists transverse confining force between the steel tube and core concrete because of their different transverse deformations. The confining force is passive, the steel and concrete are all in tri-axial stress states. This factor must be considered for the determinations of the stress-strain relations of the steel and core concrete properly.

#### 2.3.1. Stress-Strain Relations of the Steel

Figure 2 shows relations of the stress strength  $\sigma_i$  and strain strength  $\varepsilon_i$ . Details for the determinations of the parameters in Figure 2, such as  $f_y(T)$ ,  $\varepsilon_y(T)$ ,  $f_u(T)$  and  $\varepsilon_u(T)$  are found in Reference (9) and Reference(10).

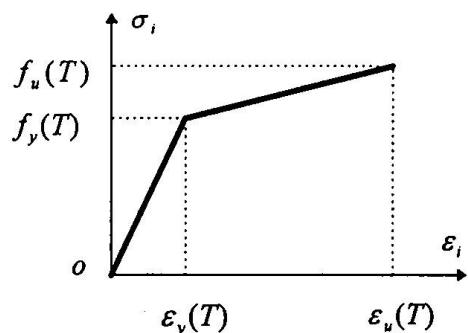


Figure 2  $\sigma_i - \varepsilon_i$  relations of the steel

### 2.3.2. Stress-Strain Relations of the Concrete

Based on the tests results of concrete filled steel tubular axial short columns under constant high temperature, the relations between longitudinal stress  $\sigma_c$  and longitudinal strain  $\varepsilon$  of the core concrete has been deduced, i.e.

If  $\varepsilon \leq \varepsilon_o$ , then,

$$\sigma_c = \sigma_o \left[ A(\varepsilon / \varepsilon_o) - B(\varepsilon / \varepsilon_o)^2 \right] \quad (1a)$$

If  $\varepsilon > \varepsilon_o$ , then,

$$\begin{aligned} \sigma_c &= \sigma_o(1 - q) + \sigma_o q (\varepsilon / \varepsilon_o)^{0.1\xi} (\xi \geq 1.12) \\ \sigma_c &= \sigma_o (\varepsilon / \varepsilon_o) / \left[ \beta (\varepsilon / \varepsilon_o - 1)^2 + (\varepsilon / \varepsilon_o) \right] (\xi < 1.12) \end{aligned} \quad (1b)$$

where,  $\sigma_o = f_{ck}(T) \left[ 1.194 + (1 - T / 1000)^{9.55} (13 / f_{ck})^{0.45} (-0.07485\xi^2 + 0.5789\xi) \right]$

$$f_{ck}(T) = f_{ck} / \left[ 1 + 1.1986(T - 20)^{3.21} \times 10^{-9} \right];$$

$$\varepsilon_o = \varepsilon_{cc}(T) + \left[ 1400 + 800 \frac{(f_{ck} - 20)}{20} \right] \xi^{0.2} (\mu\varepsilon);$$

$$\varepsilon_{cc}(T) = (1 + 0.0015T + 5 \times 10^{-6}T^2)(1300 + 14.93f_{ck})(\mu\varepsilon);$$

$$A = 2 - k; B = 1 - k; k = 0.1\xi^{0.745}; q = k / (0.2 + 0.1\xi);$$

$$\beta = (2.36 \times 10^{-5})^{[0.25 + (\xi - 0.5)^2]} f_{ck}^2 \times 5 \times 10^{-4};$$

$$\xi = \alpha f_y / f_{ck}; \alpha = A_s / A_c;$$

$A_s, A_c$  = sectional area of the steel tube and core concrete respectively;

$f_y, f_{ck}$  = strength of the steel and concrete respectively,  $f_{ck} = 0.67 \times f_{cu}$ ;

$f_{cu}$  = cubic strength of the concrete.

Composite action between the steel and its core concrete have considered in Equation(1).

### 2.3.3. Composite Stress -Strain Relations of Concrete Filled Steel Tubes

The 'composite' relations of longitudinal stress  $\bar{\sigma}$  ( $=N/As_c$ , where  $N$  is the load of axial compression,  $As_c = As + Ac$ ) and longitudinal strain  $\varepsilon$  of the concrete filled steel tube under compression can be calculated by the stress-strain relations of the steel and concrete, in the calculation, equilibrium equation of force and compatibility condition of deformations should be satisfied. Figure 3 shows a typical  $\bar{\sigma} - \varepsilon$  curve. Details of the calculation method are found in Reference(9).

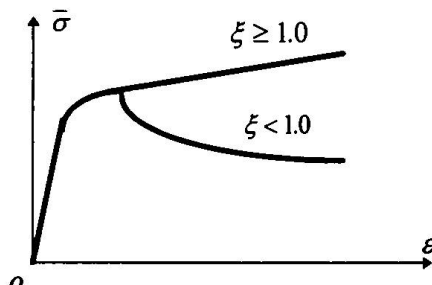


Figure 3 Typical  $\bar{\sigma} - \varepsilon$  curve

## 2.4 Calculation of Strength During Fire

The calculation of the fire resistance of the column involves the calculation of the temperatures of the fire, to which the column is exposed, the temperature in the column and its deformations and strength during the exposure to fire. Figure 4 shows deflection of the column under load of  $N$  exposure to fire,  $L$  is the length of the column,  $\phi$  is curvature at midheight of the column.

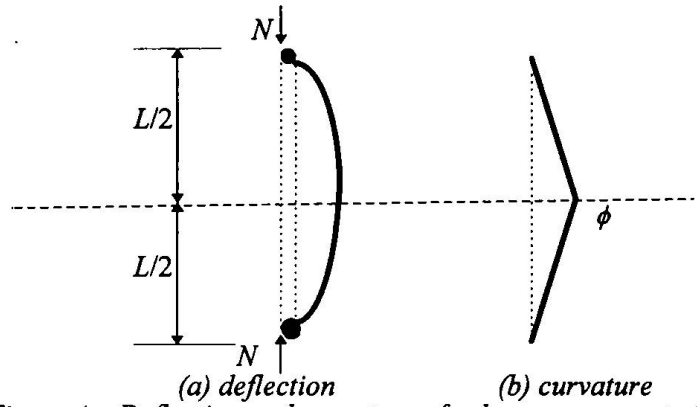


Figure 4 Deflection and curvature of column exposure to fire

Exposure to fire, the strength of the column decreased with the duration of exposure. A numerical model was worked out for the analysis of the ultimate load, the model allows a differentiated consideration of all physical and geometrical non-linearity.

In this method, for the calculation of column strength, the following assumptions were made: (1). The cross sections remain plane in the fire exposure. (2). The shape of the deformation of the member is regarded as semi-sine curve. (3). Concrete has no tensile strength. (4). the stress of the steel and concrete in compressive zone is equal to that of the concrete filled steel tubes corresponding to the same strain; the steel in tensile zone is in uni-stress state.

Based on assumption(1), the strain of the elements of the steel can be given by:

$$\varepsilon_s = \phi x_{si} + \varepsilon_o - \varepsilon_{sT} \quad (2)$$

and for the element of the concrete can be given by:

$$\varepsilon_c = \phi x_{ci} + \varepsilon_o - \varepsilon_{cT} \quad (3)$$

where,  $\varepsilon_o$  = axial strain of the column;  $\varepsilon_{sT}, \varepsilon_{cT}$  = strain of the steel and concrete due to thermal expansion;  $x_{si}, x_{ci}$  = horizontal distance from the center of the element of the steel and concrete to a vertical plane through X-AXIS of the column section respectively. The curvature  $\phi$  at midheight of the column, which can be derived from assumption(2) as follows:

$$\phi = (\pi^2 / L^2) u_m \quad (4)$$

where,  $u_m$  = deflection at midheight of the column.

Internal axial load of the column section at misheight is:

$$N_{in} = 2 \sum_{i=1}^n (\sigma_{si} dA_{si} + \sigma_{ci} dA_{ci}) \quad (5)$$

where,  $\sigma_{si}, \sigma_{ci}$  = longitudinal stresses of the steel and concrete element respectively; From assumption(3) and (4), in tensile zone of the section,  $\sigma_c = 0$ , and  $\sigma_{si}$  can be determined according to Figure 2; in compressive zone,  $\sigma_c$  can be determined according to equation(1),  $\sigma_{si}$  can be deduced as follows:

$$\sigma_{si} = [\bar{\sigma}(A_s + A_c) - \sigma_c A_c] / A_s = [\bar{\sigma}(1 + \alpha) - \sigma_c] / \alpha \quad (6)$$

Internal bending moment of the column section at midheight is:

$$M_{in} = 2 \sum_{i=1}^n (\sigma_{sli} x_{si} dA_{si} + \sigma_{cli} x_{ci} dA_{ci}) \quad (7)$$

For any given curvature  $\phi$ , and thus for any given deflection  $u_m$  at midheight of the column, the axial strain  $\varepsilon_o$  is varied until the internal moment at the midsection is in equilibrium with applied moment, which is:

$$M_{in}/N_{in} = e_o + u_m \quad (8)$$

where,  $e_o$  = initial load eccentricity, or arbitrary load eccentricity of the column.

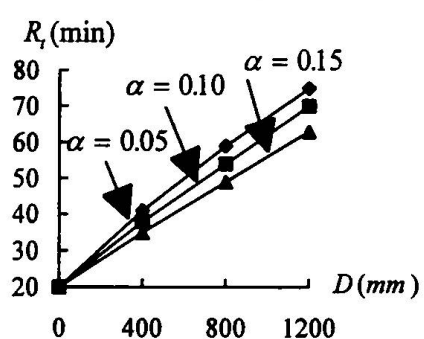
Based on the method introduced above, the strength of column during exposure to fire was calculated, there is good agreement in the trend of deformations between calculated and measured results (more details are found in Reference (9)). A current failure criterion for the column, based on the contraction and the rate of contraction, is that proposed in the ISO-834 Standard, a column is considered to have failed if the column has contracted axially by  $0.01L$  mm and the rate of contraction has reached  $0.003L/min$ . A comparison of results calculated using this method with the results of tests is shown in Table 1. There is reasonably good agreement.

TABLE 1. Comparison of Fire Resistance of Tested and Calculated

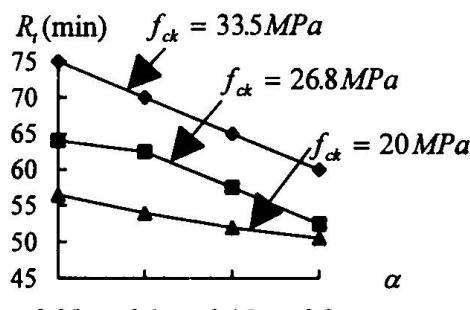
Column No.	Outer Diameter (mm)	Steel Wall Thickness (mm)	Steel Strength (MPa)	Concrete Strength (MPa)	Test Load (kN)	Fire Resistance (min) Measured <sup>[6,7]</sup>	Fire Resistance (min) Calculated
1	141.3	6.55	350	30	110	55	68
2	168.3	4.78	350	30	218	56	48
3	219.1	4.78	350	30	492	80	69
4	273.0	6.35	350	46.7	1050	188	194
5	273.0	6.35	350	47	1900	96	92
6	273.1	5.56	350	30	525	133	112
7	355.6	12.70	350	30	1050	170	168

\* There are reinforced bars in the core concrete<sup>[7]</sup>.

By the use of the analytical method, influence of the changing steel ratio ( $\alpha$ ), strength of the steel ( $f_y$ ) and of concrete ( $f_{ct}$ ), diameter ( $D$ ) of the column on the fire resistance were analyzed (see Figure 5), in the calculations the applied load of the column have been designed according to 'Designing Code of Concrete Filled Steel Tube of China (DL5400-97)', the initial arbitrary load eccentricity is taken as  $0.001L$ . Slenderness ratio ( $\lambda = 4L/D$ ) has almost no influence on the fire resistance time  $R_f$  of the column.



$$(\lambda = 20; f_y = 380 \text{ MPa}; f_{ck} = 26.8 \text{ MPa}) \quad (\lambda = 20; f_y = 380 \text{ MPa}; D = 1000 \text{ mm})$$



(b)

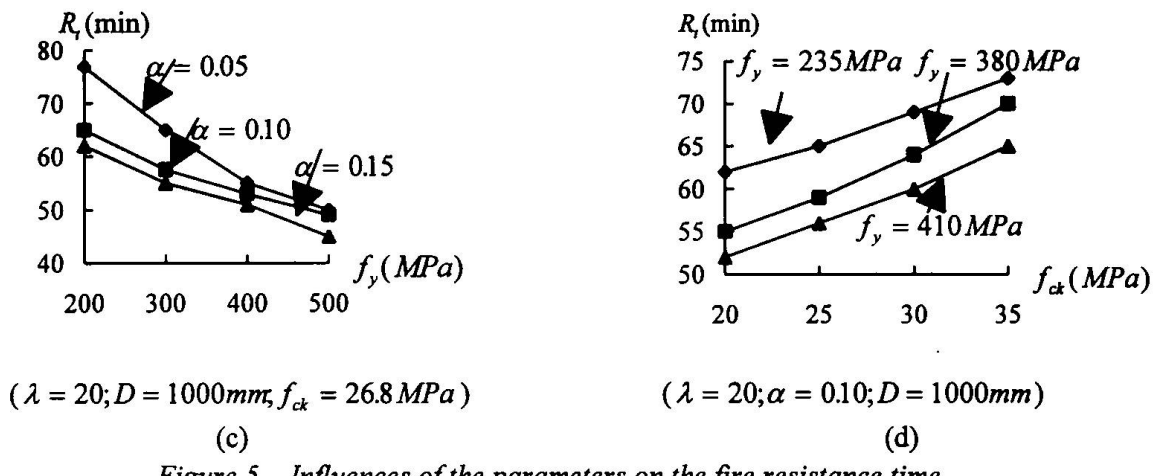


Figure 5 Influences of the parameters on the fire resistance time

### 3. Conclusion

Based on the analytical results of this study, the following conclusion can be drawn:

- (1). The analytical method introduced in this paper is capable of predicting the fire resistance of the concrete filled steel tubular columns.
- (2). There is composite action between the steel and concrete under fire. The action has been considered in the model for the calculations of the fire resistance of concrete filled steel tubular columns introduced in this paper.
- (3). Based on the results of calculation, any desired fire resistance time can be obtained depend on the type and the thickness of the isolating material.

### References

1. Design Manual for SHS Concrete Filled Columns, British Steel Corporation, Corby Technical Center, U.K., 1984.
2. Johannes Falke, Comparison of Simple Calculation Methods for the Fire Design of Composite Columns and Beams, Proc. of an Engineering Foundation Confer. on Steel-Concrete Composite Structures, New York, the Structural Division of the ASCE, 1993, pp. 226-241.
3. Timo Inha, A Simple Method for the Structural Fire Design of Composite Structures, Proc. of an Engineering Foundation Confer. on Steel-Concrete Composite Structures, New York, the Structural Division of the ASCE, 1993, pp. 210-223.
4. Klingsh, W., and Wittbecker, F. W., Fire Resistance of Hollow Section Composite Columns of Small Sections, Bergische University, Wuppertal, Germany, 1988.
5. T. T. Lie, and D. C. Stringer, Calculation of the Fire Resistance of Hollow Structural Section Columns Filled with Plain Concrete, Can. J. Civ. Eng. 21, 1994, pp. 382-385.
6. T. T. Lie, and M. Chabot, A Method to Predict the Fire Resistance of Circular Concrete Filled Hollow Steel Columns, J. of Fire Prot. Engr., 2(4), 1990, pp. 111-126.
7. T. T. Lie, Fire Resistance of Circular Concrete Filled with Bar-Reinforced Concrete, J. of the Struct. Engr., Vol. 120, No. 5, M94, pp. 1489-1509.
8. Han Lin-hai, Finite Element Analysis of Thermal Field of Concrete Filled Steel Tubes under Fire, J. of Harbin University of Civ. Eng. and Architecture, Vol. 30, N0.2, 1997.
9. Han Linhai, Fire Resistance of Concrete Filled Steel Tubular Beam-Columns, Internal Report of Chinese Nation Natural Science Foundation, Beijing, 1996.
10. Han Lin-hai and Zhong Shan-tong, Mechanics of Concrete Filled Steel Tubes, Dalian University of Technology Press, 1996.

## Fire-resistant Structure: The Concrete Filled Steel Tubular Column

**Ping-Zhou LIN**  
Senior Engineer  
CNBMI  
Hangzhou, China

Born in 1936, graduated  
from Tsinghua University  
China

**Zong-Cheng ZHU**  
Senior Engineer, E. Master  
CNBMI  
Hangzhou, China

Born in 1945, graduated  
from Nanjing University  
of Aeronautics & Astronautics,  
China

**Zhi-Jun LI**  
Senior Engineer  
CNBMI  
Suzhou, China

Born in 1931 graduated  
from North Eastern  
University, China

### Summary

The concrete filled steel tubular column for supporting a furnace at one glass factory has been firstly used in the world, with a total number of 70 columns in four rows. Hundreds of tons of high-temperature molten glass leaked out onto the ground at the bottom of the furnace columns and caused the fire. These columns had not miraculously been burnt away in the fire and had still effectively supported the furnace weight. This paper presents the fire situation, structure damaged status and mending work, and evaluates the fire-resistant characteristics of these columns.

#### 1. General situation of engineering and fire

The concrete filled steel tubular column for supporting glass furnace was firstly used at one Chinese large glass factory in 1992, and it succeeded completely. The plane size of the furnace is 50 m × 10 m. At the furnace bottom, there are 70 columns altogether, four rows, eighteen teams (figure 1). The column grid is 3 m × 4 m. Each column is 7300 mm high, Φ 245 mm, C 30 concrete used. The cross-section of the column is only 1/14 of the traditional reinforced concrete square column for 3' × 3' (914 mm × 914 mm) in size.

Unexpectedly, a crack occurred at the furnace bottom in the maximum temperature area during the process of production. Hundreds of tons of molten glass over 1300 °C leaked out for several hours. A sea of fire like magma occurred at the furnace bottom.

The fire was put out by the fire hose. After it was cold, we watched and found that the molten glass firstly leaked to the second concrete floor beside the furnace, then flowed to the ground along the plate edge of the platform. A great deal of the molten glass accumulated at the furnace side and flowed forward. The mass of leaked glass on the ground was about 1 meter thick. Another part of molten glass crossed the footpath and flowed to the other side of the furnace. The mass on the ground got thinner and thinner. The thinnest part was about 2 - 3 mm thick. The glass accumulation under the accident point reached 3m high. A concrete filled steel tubular column was casted in it (here-in-after referred to as column A). The mass around the root of another column (here-in-after referred to as column B) was almost 400 mm thick. The mass on the second concrete floor was more than 1.5 m thick. Fortunately, the whole furnace was still safe as before, even no great integral deformation occurred. This miracle sufficiently showed that the concrete filled steel tubular is one kind of fire-resistant structures.

## 2. Concrete filled steel tubular column yielded but not fell

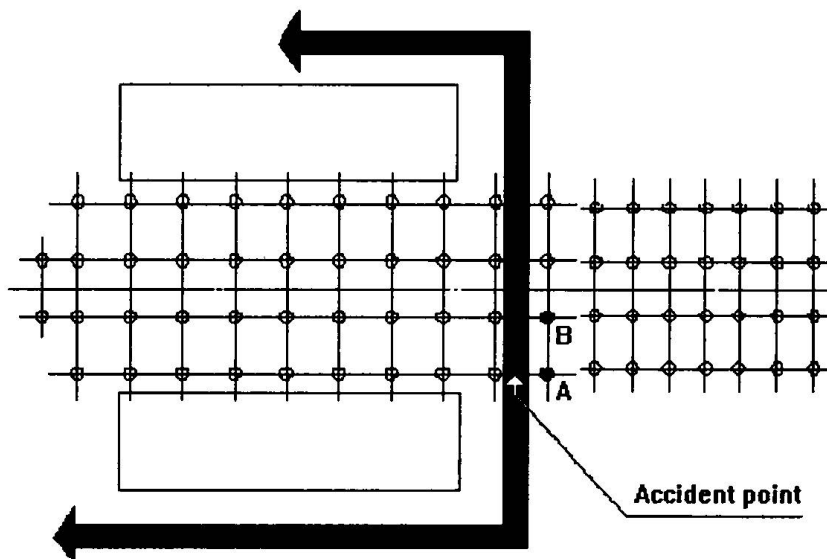


Figure 1

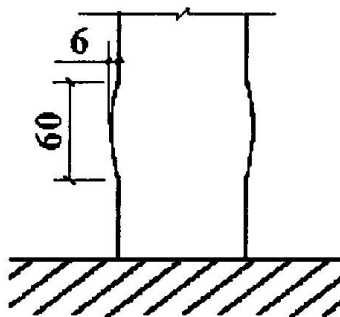


Figure 2

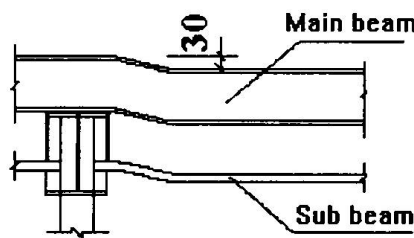


Figure 3

After cutting off the solidified glass rock which was still over 100 °C on its surface, we found that there was a circle of convex vestige at each root of column A and B which had risen because of buckling (figure 2). The convex vestige rise cylinder about 6 mm. The leaning lateral deflection of the lower part of column A was about 3.0 cm. But the two column were still supporting about 80 % of the design load acting on their top. The steel II-beam was roasted by the poured down molten glass from the accident point, and had about 3.0cm shear deformation (figure 3). The rendering and protective coating of the boundary beam on the second floor were scoured and peeled off. By the flowing molten glass, several hoop reinforcements in the boundary beam had already been faintly visible. The concrete floor slab was already map cracking and loose.

### 3. Strengthening the concrete filled steel tubular column with the concrete filled steel tubular.

We sleeved the root of column A and B with two  $\Phi 500 \text{ mm} \times 5 \text{ mm}$  semicircle steel tubes 2.5 m high, then butted and welded them together, and poured the gap with C 30 concrete. The work finished in eight hours. In addition, we added the channel steel to both side of the damaged main steel II-beam and laid them directly onto the top of column to replace the action of the former main beam. The loose concrete of the platform was cut off and repaired after the production resumed. The resumption of the normal production showed that the reinforcement we did was successful.

### 4. Time of burning more than 3 hours

Normal plate glass softens at  $700^\circ\text{C}$ , melts and flows at  $900^\circ\text{C}$ . So the temperature of molten glass flowing along the floor must be over  $1000^\circ\text{C}$ . Calculating with formula  $W = \frac{\sum Q_i}{4500A}$

<sup>[11]</sup>, the load density of the molten glass piling up about 1 m high on the ground in fire was about  $156 \text{ kg/m}^2$ . It was 3-6 times as it is in common fire. The time of burning corresponds to 3.25 hours on standard temperature rise curve line (similarly hereinafter). The average height of the glass mass on the ground about ten square meter under the accident point was about 2m, its load density in fire was over  $312 \text{ kg/m}^2$ , and its burning time was 8.40 hours. The fire-resistant limit of multiply column in first rating fire-resistant building stipulated is in 3.0 hours in China.

### 5. Unique fire-resistant supporting ability

It is well known that the cohesive force between reinforcing bar and concrete has almost been lost when the reinforced concrete structure is at  $300-400^\circ\text{C}$ .  $\text{CaSiO}_3$  decomposes to  $\text{CaO}$  and  $\text{SiO}_2$  at  $400^\circ\text{C}$  and concrete will fail permanently<sup>[11][15]</sup>. Both elastic modulus of concrete and yielding limit of steel tend towards zero at  $600^\circ\text{C}$ <sup>[12][16]</sup>. It shows that the temperature of  $400-600^\circ\text{C}$  will seriously damage the reinforced concrete structure or steel structure. In this fire, column A and B were in the state of the temperature which was far above  $600^\circ\text{C}$  for a long time. They supported more than 80% of the former design load effectively though their roots had yielded. It showed amazing fire-resistant supporting ability. The three conditions of the experiment to judge the fire-resistant limit of building structural members are supporting ability, integrity of structural members and fire division function. The concrete filled steel tubular column doesn't belong to fire division component. So it was the supporting ability that resolves the column's fire-resistant limit. Supporting ability behaves as the former intensity indication doesn't depress or depresses little, the structural deformation does not exceed preset limit and lose stability. The fact that column A and B didn't occur general meaning lose stability failure showed that the concrete filled steel tubular column had nice fire-resistant supporting ability.

### 6. Discussion about the high fire-resistant function

Currently, there is no sufficient and clear information on the experiment and evaluation about the fire-resistant function of the concrete filled steel tubular. The structural characteristics of the concrete filled steel tubular and the effect of its fire-resistant function are macroscopically discussed just from the fact in this fire:

- (1) The buckling deformation of column A and B under high temperature was similar to that of short concrete filled steel tubular column pressed by axial pressure under normal temperature in laboratory. The common ground was that the column top did not unload or unloaded little when the cross-section at column root yielded. The whole column could still keep safe and work on, and the vicious sudden failure did not occur like reinforced concrete structure or steel construction did when the cross-section yielded or the stability lost. It kept the structure safe fundamentally.

(2) The load-bearing capacity of the concrete filled steel tubular column is much higher than that of reinforced concrete or steel column with same cross-section size. At the same time, the concrete filled tubular column can fit the adverse circumstances better. Comparing the three kinds of column : the concrete filled steel tubular column  $\Phi 245 \times 8$  ( $f_y = 235 \text{ N/mm}^2$  C 30), the steel tubular column  $245 \times 8$  ( $f_y = 235 \text{ N/mm}^2$ ), the reinforced concrete circular column  $\Phi 245(12\Phi 12)$ ,  $f_y = 345 \text{ N/mm}^2$ ,  $\mu = 4.19\%$ , C 30), and calculating by 7300mm in height, the ultimate bearing capacities of the three kinds of column respectively are 1513.4 kN, 1030.2 kN, 543.3 kN. The ratio of bearing capacity of the three columns is 1 : 0.68 : 0.36. It means that the bearing capacity of the concrete filled steel tubular column is 1.47 and 2.79 times as that of the other two. The bearing capacity of the above-mentioned three columns respectively is 750.0 kN, 381.5 kN, 179.9 kN if the three columns were fixed at the bottom and 30mm horizontal displacement occurred on the top. The ratio of bearing capacity of the three columns is 1 : 0.51 : 0.24. It means that the bearing capacity of the concrete filled steel tubular column is 1.96 and 4.17 times as that of the other two. It shows that the bearing capacity of the concrete filled steel tubular column is higher than that of the other two when the horizontal displacement occurs on the column top.

(3) The surface of the concrete filled steel tubular column will not burst what matter if it met fire or water on fire. It can keep certain cross-section integrity. The harmful consequence such as the crack and exfoliation of the protective course or the twisting of steel structure cross-section will not engender.

(4) The concrete filled steel tubular column will not be damaged by the secondary disaster such as the crack on the margin of the concrete column or the concave on the steel tubular when it is collided unexpectedly on fire.

(5) The mechanical property of the yielded cross-section of the concrete filled steel tubular will be improved greatly along with the decrease of the external temperature. Its main reason is that a certain the strength of steel tubular recovers and the structure integrity increases greatly than it is on fire. It supplies fairly safe working environment to strengthen the structure. It also reduce the working capacity of strengthening. While the mechanical property of the cross-section and the structure integrity of the reinforced concrete structure which has modified and cracked in high temperature can not be recovered or improved along with the decrease of the external temperature. The lost stability or twisted member of steel structure can not bring any more safety to structure in normal temperature, too.

(6) The yielded cross-section of column B was at the column root, it perhaps relates to the characteristics of this fire. But about 3m high of lower part of column A has been covered with melted glass, and its yielded cross-section was at the root too. All other cross-sections of column A was in good condition. This phenomenon probably means that the most dangerous cross-section of the internal force for concrete filled steel tubular structure will be the firstly yielded cross-section in fire. It perhaps indicates that the position of the yield cross-section uncertainly relies on the specific location of fire distribution. It also can supply a chance for designers to foresee and take prevention, thus the designers can improve the fire-resistant function directly. The fact that the concrete on platform lost widely shows that the cross-section position where the concrete material had modified and cracked depends on the distribution of the fire, and not certainly at the most dangerous cross-section of internal force. So it is fairly undefined.

(7) The point that should be put forward is that the diameter of this concrete filled steel tubular column is only 245mm because of the particularity of the design load in this engineering. It is one kind of small diameter, large slenderness ratio columns which is very seldom used in engineering. The fire-resistant supporting time of short or middle length columns with larger diameter which are widely used will improve greatly.

## 7. Conclusion

The fire was a real test for the concrete filled steel tubular columns. Although this fire was very particular, its result was quite valuable. The fact shows that the concrete filled steel tubular column is one kind of fire-resistant construction, and has wide developing field. Its fire-resistant limit should be measured on the scientific experiment so as to direct design work. It has a great practice significance to research the load effectiveness of the concrete filled steel tubular structure on fire.

Leere Seite  
Blank page  
Page vide

## Fire Resistance of Timber-Concrete Composite Slabs

**Mario FONTANA**  
 Professor  
 ETH Zürich  
 Zurich, Switzerland

**Andrea FRANGI**  
 Civil Engineer  
 ETH Zürich  
 Zurich, Switzerland

### Summary

The use of timber in multi-storey buildings is limited due to fire regulations. Timber-concrete composite elements show promise to overcome this handicap thus cutting down on the use of the sustainable building material timber. A research project at ETH on the fire behaviour of timber-concrete composite slabs is described.

### 1. Design and application of timber-concrete composite slabs

A rigid connection between concrete slabs and timber beams improves the serviceability and resistance of such floors. In Europe the refurbishment of old buildings with timber floors has drawn attention to this new and efficient floor system in recent years. Fig. 1 shows a traditional timber floor with slag filling between the beams and the new type of timber-concrete composite slabs after refurbishment. Beams and planks are reused and the slag is replaced by (preferably lightweight) concrete. If the planks have deteriorated over the years they can be replaced by profiled steel sheets, timber boards or wood-based panels.

As timber-concrete composite floors show excellent behaviour with regard to serviceability, resistance, noise insulation and fire resistance, they are not only used for refurbishment but also for new slabs in dwellings and public buildings in Europe. Besides the beam type floors, slab type floors using laminated wood decks of sawn timber planks nailed together with the longer side of their cross-section vertical or glued laminated beams with the longer side of their cross-section horizontal are common (fig. 2). They create a pleasant looking ceiling for the room below.

The behaviour of timber-concrete composite slabs is governed by the shear connection between timber and concrete. Because timber exhibits brittle behaviour (no yield plateau as for steel) only elastic design methods can be applied. Fig. 3 shows the influence of the shear connector stiffness on the stress distribution. Table 1 gives an example of timber-concrete composite beam of 6 m span, a permanent load of  $2 \text{ kN/m}^2$  and a live load of  $2 \text{ kN/m}^2$ . The connectors have a stiffness of  $13 \text{ kN/mm}$  and are spaced 90 mm. Propping of the beam during the concrete setting is crucial for the efficiency of timber-concrete composite floors.

The Annex B of Eurocode 5 [1] gives a simplified design method applicable to simply supported beams with uniform loads. For more general boundary conditions nonlinear finite element analysis needs to be performed because the differential equation has no general solution for such cases. A finite element program taking into account even thermal action in the case of fire is currently being developed at our institute by Prof. Dr. E Anderheggen and his team.

As the shear connectors markedly influence the efficiency of timber-concrete composite slabs many forms of connectors have been developed and tested during the last years. From the variety of connectors two types (figs. 4 and 5) are being tested in an ongoing research project at our institute sponsored by the industrial partners SFS, Hilti and Lignum and the Swiss Commission for Technology Transfer and Innovation. The Hilti connector (fig. 4) was developed together with the Institute of Timber Construction (IBOIS) at the ETH in Lausanne. It consists of a glued threaded bar M12 which is post-tensioned after the setting of the concrete to improve the stiffness. The shear is transferred by grooves perpendicular to the span [7].

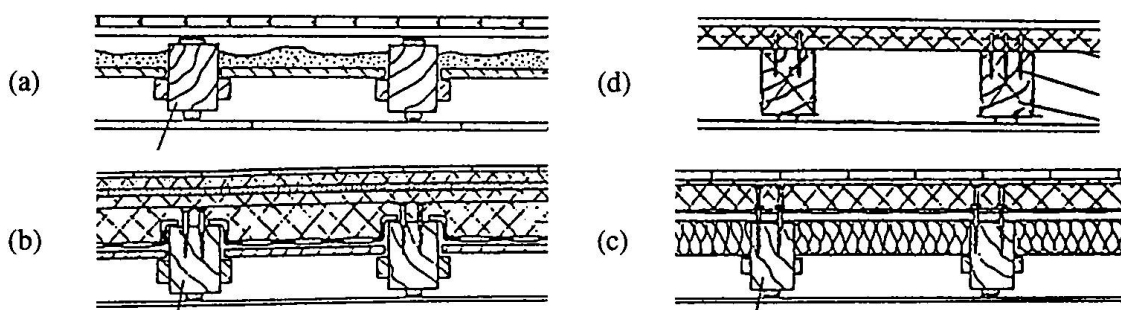


Fig. 1 Typical traditional timber floor (a) and three types of refurbishment as timber-concrete composite slabs using the existing planks (b) or a new timber board (c) or steel deck (d)

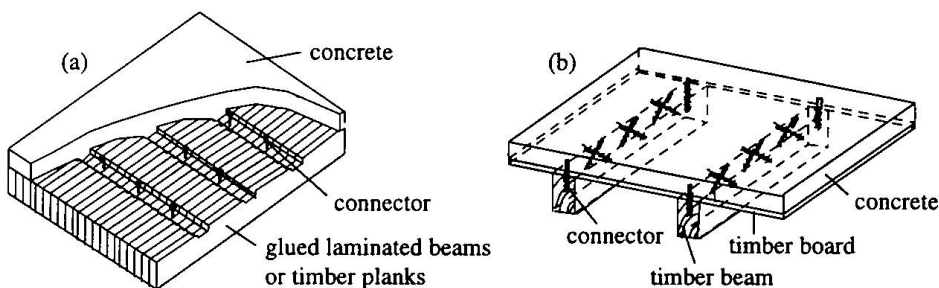


Fig. 2 Design of timber-concrete composite floors: slab type floor (a) made of glued laminated beams with the longer side of their cross-section horizontal or nailed laminated wood of sawn timber planks and beam type floor (b) with glued laminated or sawn sections

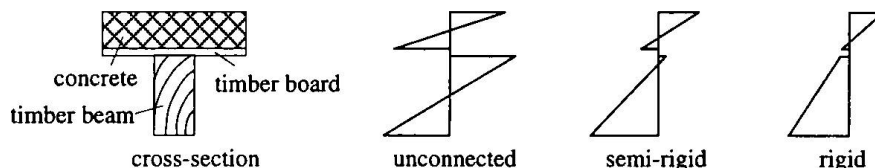


Fig. 3 The stiffness of the shear connection has a marked influence on the stress distribution and the efficiency of timber-concrete composite slabs

		(a) unpropped			(b) propped	
		unconnected	semi-rigid	rigid	semi-rigid	rigid
mid-span-deflection (longterm inside building)		70 mm	27 mm	25 mm	13 mm	11 mm
maximum longterm tensile stress in timber		16.6 N/mm <sup>2</sup>	9.7 N/mm <sup>2</sup>	9.4 N/mm <sup>2</sup>	4.9 N/mm <sup>2</sup>	4.4 N/mm <sup>2</sup>

Table 1 Example of deflection and stress in a timber-concrete composite beam. The construction process (propped/unpropped) and the rigidity of the connectors are important parameters

The SFS connector VB-48-7.5x100 (fig. 5) is a self-drilling screw with a collar to limit the screwing depth and a head for connection with the concrete. The net section in the threaded part has a diameter of 4 mm, the upper part of the connector a diameter of 6 mm. By arranging the connectors at 45° inclination a virtual truss is formed with the timber and the concrete as girders and the connectors as diagonals. Such an arrangement improves the stiffness by a factor of 3 compared to a vertical arrangement where the connector acts in bending and bearing [6].

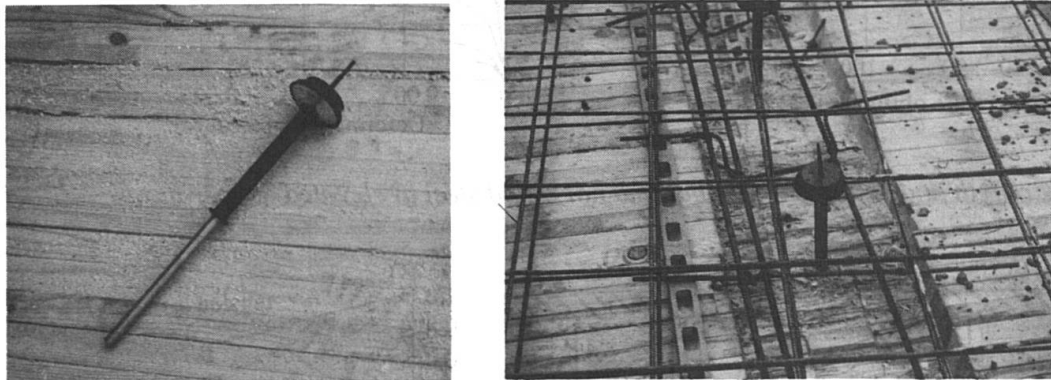


Fig. 4 Hilti connector. It consists of a glued threaded bar M12 which is post-tensioned after the setting of the concrete. The shear is transferred by grooves perpendicular to the span

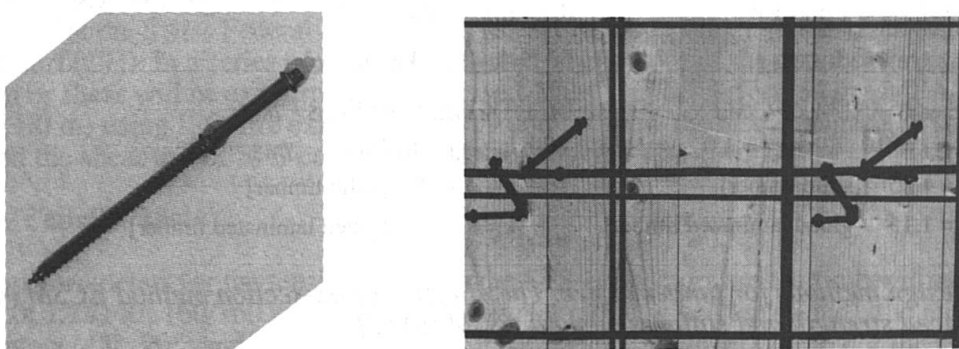


Fig. 5 SFS connector. It consists of a self-drilling screw with a collar to limit the screwing depth and a head for connection with the concrete.

## 2. Fire resistance of timber-concrete composite slabs

The fire resistance of timber-concrete composite elements is mainly influenced by the behaviour of the timber and the connectors. Timber is a combustible material and if heated the decay of cellulose and lignin produces combustible gases and charcoal. The burning rate is mainly influenced by the specific density, the moisture content, the thermal conductivity and specific heat capacity. In a room fire the heat flux will influence the burning rate so that the fire behaviour is a rather complex phenomenon. For design purposes a simplified method based on a constant burning rate is commonly used. The fire reduces the cross-section and the stiffness and strength of the timber close to the burning surface. Fig. 6 shows the reduction of stiffness and strength for timber [3] and of the yield stress of steel [4].

The simplified design methods consider the strength and stiffness reduction either by a) an effective cross section (ECSM) e.g. adding an additional depth to the charred depth or b) by a general reduction of stiffness and strength for the residual section depending on the ratio between the exposed boundary  $p$  and the residual section  $A_r$  (RSSM). More sophisticated methods also consider the higher charring in the corners which leads to a „rounding“ of the corners in fire [2].

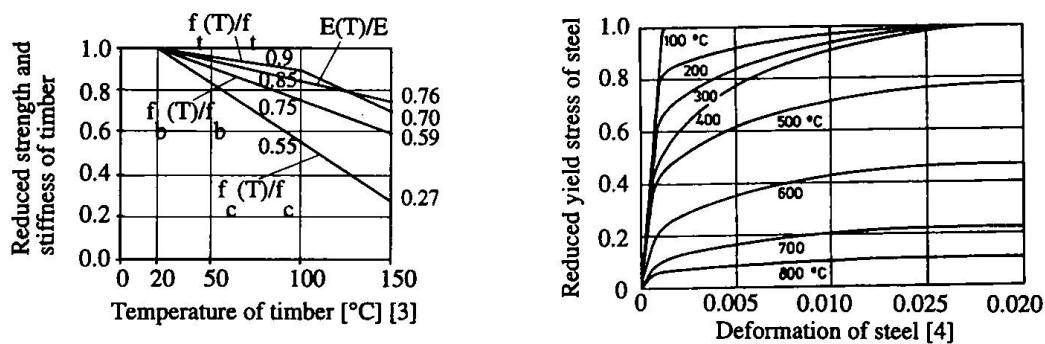


Fig. 6 Reduced strength and stiffness for timber and hot rolled steel at elevated temperatures

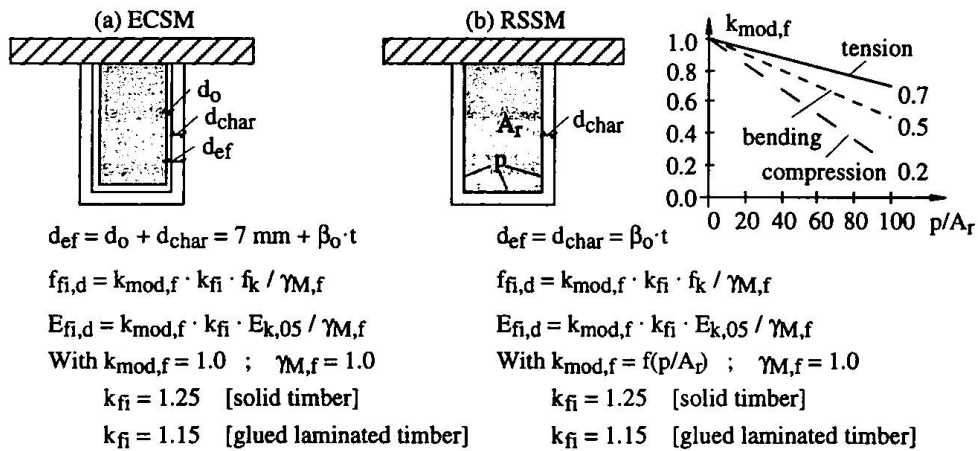


Fig. 7 Simplified design methods for timber in fire. The effective cross-section method ECSM (a) and the reduced strength and stiffness method RSSM (b) [2]

For timber-concrete composite floors the strength and stiffness reduction of the connectors and the thermal stresses between timber and concrete have to be considered. It is the aim of the ongoing research project to investigate these parameters. The temperature distribution in the timber and concrete section is an important parameter. The temperature field analysis is based on the differential equation of the transient heating process.

$$\frac{\partial \vartheta}{\partial t} = \frac{\lambda}{c \cdot \rho} \cdot \left[ \frac{\partial^2 \vartheta}{\partial x^2} + \frac{\partial^2 \vartheta}{\partial y^2} \right] \quad \text{With} \quad \begin{aligned} \vartheta &= \text{temperature} & x, y &= \text{coordinates} \\ \lambda &= \text{thermal conductivity} & \rho &= \text{specific density} \\ c &= \text{specific heat capacity} \end{aligned}$$

For the analysis of standard fire tests the surrounding temperature is given by the standard fire curve according to ISO 834. The heat transfer is mostly considered by constant values for the resultant emissivity  $\epsilon_{\text{res}}$  and the coefficient of heat transfer by convection  $\alpha_c$ . Thermal conductivity and specific heat capacity of wood are a function of the temperature (fig. 8). The peak in the specific heat at 100°C results from the dissipation of energy due to the vaporisation of water (moisture content of 10%). Temperature field calculations in timber sections are usually based on a finite element analysis [8]. With increasing temperature the timber transforms into charcoal and later disappears. This phenomenon is simplified in the programs by gradually changing the thermal properties of wood into those of charcoal and finally into those of air with increasing temperature.

Temperatures of more than 50 to 80°C (depending on the type of glue) may affect the strength of the glue and the shear strength of the timber close to the connection [9]. A sufficient cover of the connectors is therefore important. In the fire situation the reinforcement of the concrete used for crack control in the cold situation can make an important contribution to the fire resistance as it is

insulated by the timber especially in wood laminated slabs. The beneficial effects of such global behaviour will also be investigated within the research project.

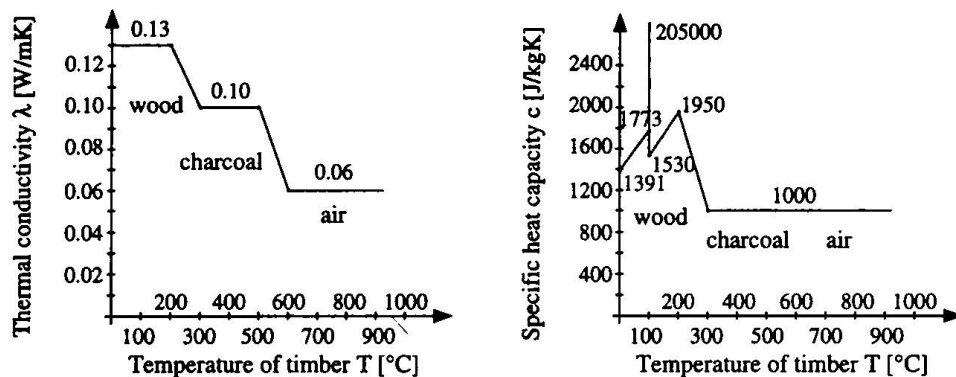


Fig. 8 Thermal conductivity and specific heat capacity of wood as a function of the temperature

### 3. Fire tests

An extensive testing program is planned to enlarge the experimental background of the design models for the fire resistance of timber-concrete composite floors. All fire tests are being performed at the Swiss Federal Laboratories for Materials Testing and Research (EMPA) in Dübendorf (CH). In a series of small scale tests the behaviour of the connectors subjected to tension or shear will be experimentally analysed. They will be performed in EMPA's small furnace (1.2 x 1.0 m) using ISO-fire exposure. Figs. 9 and 10 show the test arrangement for the tensile test and the shear test of SFS-connectors subjected to the ISO-fire.

#### 3.1 Tensile tests

The test parameters for the tensile tests with the SFS-connectors are the timber dimensions (80/120; 120/140; 160/160 mm), the type of timber (solid, glued laminated), the inclination of connectors (45°; 90°) and the gap between timber beam and timber board. For the Hilti-connectors with slab type floors the influence of the timber cover of the connector at the bottom (20, 40, 60 mm) and the type of planks (sawn, planed, glued laminated) are varied, whereas for the beam type floors with Hilti-connectors the timber dimensions (80/90; 80/100; 80/120; 120/140; 160/160 mm) and the type of timber (timber, glued laminated) are changing parameters. In the tests the temperature in selected locations, the deformation of the connectors and the tensile force are measured.

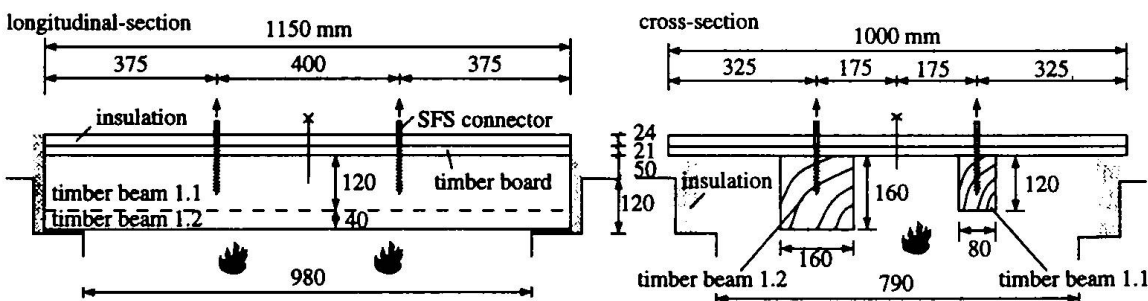


Fig. 9 Test arrangement for the tensile test of SFS-connectors subjected to the ISO-fire

The tests will be performed using two different procedures:

- The specimens are exposed to 30 minutes of the ISO-fire with the permissible load applied to the connectors. If no failure has occurred after 30 minutes the load is increased until failure occurs.
- The specimens are loaded with the permissible load and then exposed to ISO-fire until failure.

### 3.2 Shear tests

The test parameters for the shear tests with the SFS-connectors are the timber dimensions (80/120; 120/140; 160/160 mm) and the type of timber (timber, glued laminated). For the Hilti-connectors with slab type floors the influence of the timber cover of the connector at the bottom (20, 40, 60 mm) and the type of planks (sawn, planed, glued laminated) are analysed. For the beam type floors with Hilti-connectors the timber dimensions (80/110; 80/120; 80/140; 120/160; 160/180 mm) and the type of timber (solid, glued laminated) are varied.

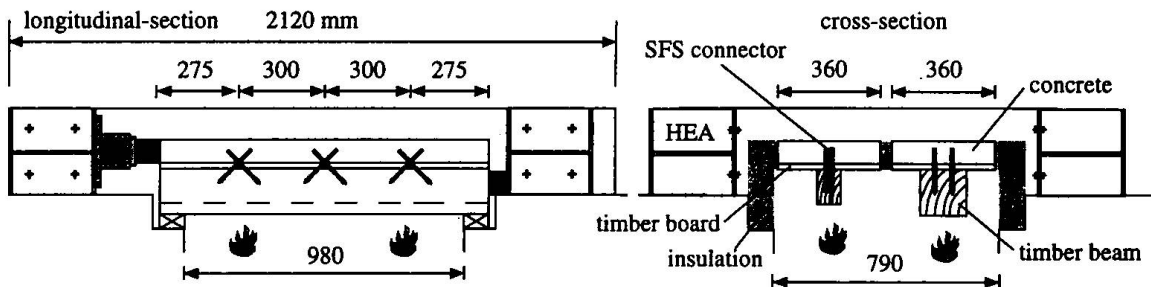


Fig.10 Test arrangement for shear test of SFS-connectors subjected to the ISO-fire

The test procedures follow the same principles as for the tensile tests. The relative deformation and the temperatures in selected locations are measured. Results of the tensile and shear tests are expected to be available in summer 1997.

A series of fire tests on slabs (3.0 x 5.0 m) is planned for the end of 1997, which will look at the global behaviour of timber-concrete composite slabs. The research project should lead to construction details improving the fire resistance of timber-concrete composite elements and form a background for a new consideration of the application of timber in multi-storey buildings by the fire authorities and for a liberalisation of the present fire regulations for timber-concrete composite construction. This should then lead to new markets for timber in multi-storey buildings.

## 4. Bibliography

- [1] ENV 1995-1-1 „Eurocode 5“: Design of timber structures, Part 1-1 General rules and rules for buildings, 1993
- [2] ENV 1995-1-2 „Eurocode 5“: Design of timber structures, Part 1-2 General rules, supplementary rules for structural fire design, 1994
- [3] Deutsche Gesellschaft für Holzforschung e.V., Holz-Brandschutz-Handbuch, 2 Auflage, K. Kordina, C. Meyer-Ottens, C. Scheer, 1994, Ernst & Sohn
- [4] R. Hass, C. Meyer-Ottens, E. Richter, Stahlbau-Brandschutz-Handbuch, 1994, Ernst & Sohn
- [5] H.J. Blass, J. Ehlbeck, M.L.R. van der Linden und M. Schlager, Trag- und Verformungsverhalten von Holz-Beton-Verbundkonstruktionen, Forschungsbericht T 2710, Abteilung Ingenieurholzbau, Universität Karlsruhe, 1995
- [6] Empa, Abteilung 155, Holz-Beton-Verbundkonstruktionen, Untersuchungen und Entwicklungen zum mechanischen Verbund von Holz und Beton, K. Timmermann, U. Meierhofer, Forschungsbericht 115/30, Oktober 1993
- [7] Schulungszentrum TFB, Wildegg, Fachtagung 1007, Konzept, Berechnung und Bemessung von Holz-Beton-Verbundkonstruktionen, 1995
- [8] J. Becker, H. Bizri, B. Bresler, Fires-T, A computer Program for the Fire Response of Structures-Thermal. Fire Research Group, University of California, Berkeley, 1974
- [9] D.J. Barber, Dr. A.H. Buchanan, Fire Resistance of Epoxied Steel Rods in Glulam Timber, Research Report 94/1, Department of Civil Engineering, University of Canterbury, Christchurch, New Zealand

## Some Remarks on the Design of Timber Composite Structures Exposed to Fire

**Maurizio PIAZZA**  
 Assoc. Professor  
 University of Trento  
 Trento, Italy

Maurizio Piazza, born 1953, engineer, is Professor of Timber Structures at University of Trento. He carried out researches on steel and timber structures, on fire performance of load-bearing elements and on techniques for the static restoration of timber structures.

**Sergio CONT**  
 First Researcher  
 C.N.R.  
 Trento, Italy

Sergio Cont, born 1938, graduate in industrial chemistry, is responsible for Fire Laboratory of Wood Technology Institute (S.Michele A./Trento). He carried out researches on wood fire behaviour, fire retardant treatments, fire performance of load- and non-load-bearing elements.

**Paolo ZANON**  
 Professor  
 University of Trento  
 Trento, Italy

Paolo Zanon, born 1950, is full professor of Theory of Structures. His current work of research is mainly devoted to semirigid steel connections, partially restrained steel frames and timber structures.

### Summary

When a timber-based composite structure is exposed to fire, it is of primary importance to know the changes of the stiffness that the single component elements are subject to, especially due to the decrease in resistant sections. On the basis of some physical tests and numerical simulations carried out, it is shown that the knowledge of the static performance of a timber-based composite structure during fire needs a sufficiently accurate determination of the bending stiffness of beams and slabs, therefore of the thermal decay of timber elements; it is shown that some standards' decay models are unable to accurately predict the behaviour of those composite structures.

### 1. Foreword

Composite timber structures have been proposed and successfully experimented for a long time, also for strengthening existing timber elements, frequently suffering for various kinds of static deficiencies (material decay, inadequate resistance and stiffness). Among these, the wood-concrete mixed structures are worthy of note for newly built-houses too, since some quality criteria (fire resistance, sound proofing, vibration control) are easily fulfilled by the wood-concrete systems used as floor structures [4, 5]. It is widely accepted that the distribution of stresses between the component elements is strongly influenced by the stiffness (flexural and axial) of the component elements themselves and of the connection systems [6]. When the structure is exposed to fire, it is of primary importance to know the changes of the stiffness that the single component elements are subject to, due to a decrease in resistant sections (timber) or to variations in the mechanical parameter values which characterise them (timber, concrete, connector). This information is required in order to be able to set prediction mathematical models for the behaviour of the composite timber structures exposed to fire and particularly to determine their resistance to fire, relative to the load bearing capacity.

Significant results, coming from some tests in furnaces on full-size models of timber composite floors, are discussed and some proposals are given regarding both the simplified numerical models used to provide an adequate simulation of the real behaviour of those structures exposed to fire and the design criteria to improve their resistance under fire. To this end, *insulation* and *integrity* requirements, which have to be guaranteed by the structure in accordance with the current standards, should not be forgotten. Also on the basis of those physical tests and the numerical simulations carried out, it is clearly shown that the knowledge of the composite structure static performance during a fire needs a sufficiently accurate determination of the flexural behaviour of beams and slabs and, therefore, of the thermal decay of timber elements. It is also evident that some decay models proposed by standards are unable to accurately predict the behaviour of such timber-based composite structures.

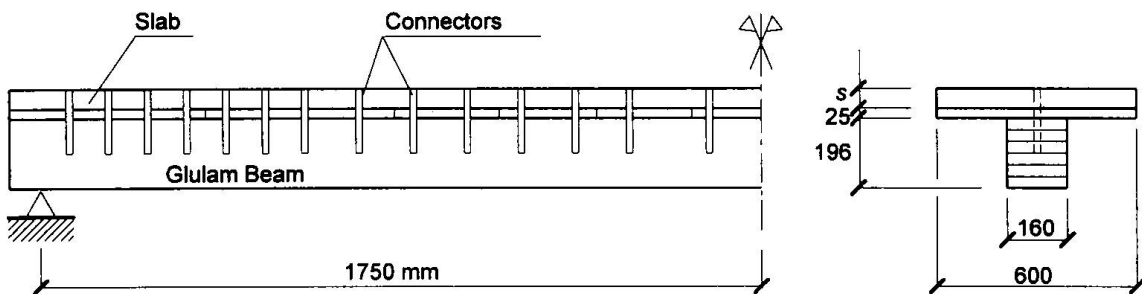


Fig. 1 - Full size samples of the tested timber-based composite structure.

## 2. Experimental Part

### 2.1 Test Samples

Tests were carried out on four timber-based composite structures, made with glulam timber beams of spruce (*Picea abies Karst.*), from the same production lot, with a cross-section of 160 x 196 mm. Such a choice was compulsory in order to achieve consistent data from the point of view of thermal decay. Elastic modulus characterization tests were, of course, carried out on each single beam as well as on the assembled composite structures, prior to the physical tests inside the furnace. These tests made also it possible to accurately check at room temperature the numerical model used for the structure's static analysis. The length of each structure is equal to  $\approx 3.50$  m, the centre distance between timber beams of the floor (slab width of the specimen) is equal to 0.60 m (Fig. 1). All samples were assembled by means of glued steel connectors [7], except the S3 specimen for which screws\* (inserted without pre-drilling) were used. Some single timber beams<sup>(1)</sup> were also tested for comparison purpose (Table I).

Model Id.	Slab		Connectors		Test Load $P_{sl}$	
	Type	Thickness $s$ (mm)	$\emptyset$ (mm)	Pitch (mm)	$P_{sl}$ (kN)	$q_{sl}$ (kN·m $^{-2}$ )
S1	Concrete	50	14	140÷220	13.66	13.01
S2	Laminated Wood Panel	48	14	100÷200	12.53	11.93
S3	Laminated Wood Panel	48*	4*	30÷90*	9.15	8.71
S4	Plywood Board	80	14	100÷200	12.55	11.96
Beam <sup>(1)</sup>	—	—	—	—	4.20	3.96

Table I - Full size models of different timber-based composite structures.

### 2.2 Testing Equipment

The tests were performed inside a furnace normally used for fire-resistance tests on elements to be exposed vertically to fire, especially equipped for performing fire-resistance tests also on load-bearing elements normally installed horizontally. The furnace consists mainly of a combustion chamber 3.00 m wide by 3.00 m high by 1.00 m in depth; the entry opening is closed-off by means of a special wall, consisting of a strong outer frame filled in with heat resistant bricks, 150 mm thick, according to the elements to be assembled and tested. The wall is assembled on a trolley so the furnace can be opened quickly at the end of the test and the fire on the tested element can be extinguished and stopped with a jet of water or other means. Heating of the furnace, depending on the selected heating programme, is accomplished using 9 natural gas radiant burners, with flames no longer than 20 cm, arranged on the bottom wall, in front of the element to be tested. The instruments located outside the furnace include a temperature programmer, a pressure regulator that operates the flue gate, a temperature recorder with a 0÷1300 °C scale, a computer for the acquisition and visualisation of all temperature, pressure and displacement data.

## 2.3 Testing Procedures

Each element to be tested is assembled diagonally inside the furnace, in order to exploit the maximum possible length ( $l=3.50$  m), with one side against the closing wall, so that only three sides are exposed to fire. The supporting system comprises two counter plates tightly fitted to both ends with a threaded bar, bolted to the external counter frame and adequately insulated. The element is loaded in the centre line by means of a special transmission pin that goes through the wall and connects to an external lever mechanism fixed to the counter frame.

### 2.3.1 Thermal action and duration of tests

The furnace was heated according to the heating programme of the international ISO 834 (1975) standard:  $T-T_0 = 345 \cdot \log_{10}(8 \cdot t + 1)$ , where  $T$  is the temperature and  $t$  the time (minutes). The fire tests were extended for about 60 minutes, therefore permitting investigations on the timber floor elements after fire (the so-called "residual" structures).

### 2.3.2 Load conditions

The proposed structures have been designed on the basis of some numerical analyses (i.e. by the F.E. model described in [5, 6, 3]); it was imposed, for all the timber beams under real test condition, a value equal to  $\approx 5.0$  MPa for the maximum stress at the beam section's lower fibre. This initial stress state could be assumed as probably being present in correspondence with a fire event. Table I gives data relative to the distributed loads  $q_{sl}$  equivalent (for the value of maximum bending moment) to the concentrated loads  $P_{sl}$  applied during the fire tests inside the furnace. It is worthy of note that all the timber-based composite structures with glued steel connectors exhibit load values  $\approx 3$  times the one shown by the single timber beam. According to current simplified calculation criteria [2] and with a charring rate  $\beta_0 = 0.7$  mm/min, the same "residual" beams, after 60 minutes exposure to fire, present maximum stress values that are still feasible (about 13 MPa). It is to be noted that, for the single timber beam, the stress value of 13 MPa (after exposure to fire) determined the load value constant during the fire test.

## 3. Experimental Results and Numerical Models

The physical data collected during each fire test included temperature data (inside the furnace, on the slab to quantify the degree of insulation provided by each floor, in the connectors to see that the temperature threshold, at which point the glue softens, was not exceeded and inside the timber beam at different depths) and floor displacements (see [3]): this was done not only for checking the mathematical models, but also for comparing similar models with those proposed by current standards, in particular ENV 1995 [1] and Italian U.N.I. 9504 [2]. Due to lack of space, only the diagrams of maximum temperatures read on the top surface of the slabs are reported in Fig. 2, as a function of time (in seconds). At a first glance, it is immediately evident how the floor comprising a concrete slab (50 mm thick) and wooden boards (25 mm) is also able to guarantee the insulation requirement with sufficient safety for 60 minutes exposure to fire ( $T_{max}=105$  °C). The same result could be obtained by the concrete slab alone, but with a  $\approx 100$  mm thickness.

Numerical modelling of composite floors' behaviour to fire, like those referred to, must principally concerns two aspects: modelling the structure's static behaviour and modelling the section's thermal decay process. As far as the first aspect is concerned, direct reference is made to the flexible connection composite structures' analysis model, already presented on other occasions [6]: remember that the beam and the slab (and also, generally speaking, the connection itself) vary during exposure to fire (geometry or mechanical characteristics). As far as concerns thermal decay models of timber section during a fire, three models are here presented, of which two from standards and one proposed by the authors. The first model is the one proposed as the "effective cross-section method" by ENV 1995 [1], the other is the one proposed by current Italian standard [2] referring only to the charring process; for both these models  $\beta_0 = 0.7$  mm/min for softwood glulam. Research up till now has made it possible to highlight the decay phenomena of the wood's mechanical characteristics in a layer under the charred surface, due to the high temperatures present ( $>100$  °C). Such phenomena, partly responsible for the decrease of stiffness beyond the theoretical value achieved on a standards basis, can still be found on residual specimens under post-fire conditions.

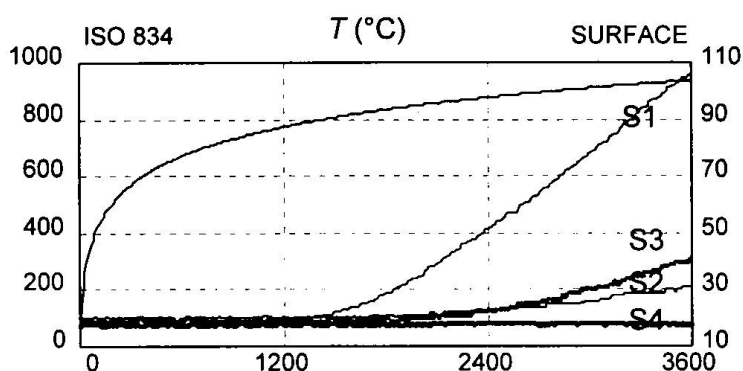


Fig. 2 - Maximum temperatures at the unexposed floor surfaces.

investigated further still also, and above all, at a microstructure point of view and assuming that the charring rate values proposed by various standards are valid, it can be assumed to be limited to a layer immediately beneath the charred one. The results of characterisation mechanical tests run up to now on residual elements (both single and composite), appear to confirm the values ranging from 2 to 5 mm in thickness of highly decayed material, under the charred layer.

The simplified cross-section of timber beam for the "engineering" type decay model, used to simulate the physical tests that have been carried out up till now, could possibly be that proposed in Fig. 3. The following variables are given in the same figure:

- $d_{ef} = d_{char} + d_{add}$ , where  $d_{add} = d_r$  (during fire) or  $d_{add} = d_i$  (after fire, at room temperature);
- $d_i$  = thickness of the layer subject only to irreversible decay phenomena;
- $d_r$  = thickness of the layer subject to irreversible and reversible decay phenomena.

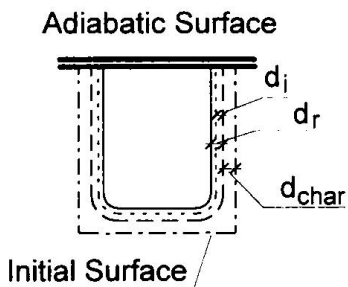


Fig. 3 - The "effective cross-section" method [1], applied also for the residual timber section.

of composite structures that were being studied. The excellent behaviour of the simple decay model described above, can be seen clearly in Fig. 4, where curves *a* (according to [2]), curves *b* (according to the "effective cross section" method of ref. [1]) and, lastly, curves *c* (according to the decay model of Fig. 3) are compared with experimental curves *Exp*. As it can be seen, the decay models currently proposed by standards and based only upon the assumption of a charring rate [2] are unable to predict the behaviour of a composite structure during a fire.

It can be of a certain interest to analyse the static behaviour of the composite structure with reference to the values of a parameter  $\gamma$  suitable to synthetically describe the static efficiency of the connection [7]. The parameter  $\gamma_{sl}$ , to which it seems appropriate the name *efficiency* with regard to serviceability limit states, can be expressed by means of the following equation:

In fact, the behaviour of a "residual" timber structure (once the charred layer has been removed completely down to the bare wood) still does not correspond to the assumed initial mechanical parameters for the whole residual section. On the other hand, the displacement values present at the end of a furnace test, differ from those found for the residual structure, but tested at room temperature. As regards the so-called irreversible decay phenomenon, it should be

investigated further still also, and above all, at a microstructure level. However, from an engineering point of view and assuming that the charring rate values proposed by various standards are valid, it can be assumed to be limited to a layer immediately beneath the charred one. The results of characterisation mechanical tests run up to now on residual elements (both single and composite), appear to confirm the values ranging from 2 to 5 mm in thickness of highly decayed material, under the charred layer.

The actual values assumed by the quantities given, depend on the several variables involved and on the dimensions of the timber beam itself (or on the *S/V* ratio between fire-exposed surface and volume of heated material). This highly simplified model could be of immediate use, having to remove from the standard's charred layer another layer, which has a constant value at least from a certain time of exposure to fire ( $\approx 20 \div 30$  minutes). The bending stiffness parameter ( $E \cdot J$ ) is, therefore, found starting from a fictitious notional section but the modulus of elasticity  $E$  is constant (equal to the initial value at room temperature). In this investigation, such a model has been set on the basis of some fire tests on single timber beams; it was later verified also on different types

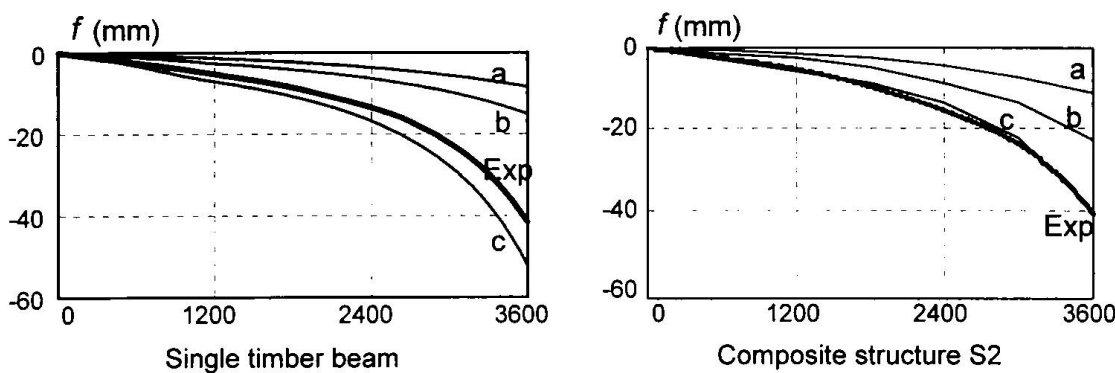


Fig. 4 - Diagrams deflection vs. time (seconds).

$$\gamma_{sl} = \frac{(E \cdot J)^* - (E \cdot J)_b}{(E \cdot J)_\infty - (E \cdot J)_b} . \quad (1)$$

The parameters  $(E \cdot J)$  in the preceding formula are the bending stiffness of the beams simply in parallel (suffix  $b$ ), of the composite beams with rigid connection (suffix  $\infty$ ) or with the actual connection (apex  $*$ ) at the same service load. The limit values of  $\gamma$  are recognisable for the value  $\gamma=0$  (connection with no stiffness) and for  $\gamma=1$  (rigid connection). It is to be noted that the values of the parameter  $\gamma$  are to be referred to a particular loading arrangement and to a specific load value. If the real displacement values are analysed for the composite structures under investigation before and after the fire test, without variation of loads, the diagram in Fig. 5 can be obtained. The *efficiency* of the connection at service load  $\gamma_{sl}$  has increased for all structures and this is a direct consequence of the connection behaviour, nearly unchanged during the fire event as imposed at the design phase, and of the simultaneous remarkable decay of timber beams.

Fig. 5 - Values of the parameter  $\gamma_{sl}$  before and after the fire event.

As regards the behaviour of the so-called *residual* structure after fire, Table II shows the values of the equivalent distributed loads  $q_u$  at failure, determined by means of mechanical tests at room temperature under the same loading arrangement, compared with the values  $q_{sl}$  kept constant during fire test. The values of  $q_u$  demonstrate that the problem of evaluating the structure's residual resistance subsequent to a non-destructive fire event is of fundamental importance especially for timber-based composite structures.

With reference to the design phase and to the material partial safety factor imposed for the bending strength of timber element after fire, it can be noted that only the composite structures with high values of the initial static efficiency ( $S_1, S_2, S_4$ ) are able to exhibit values of safety factor for the whole structure greater than the initial one. This is a consequence of the material's anisotropy characteristics and the random defects inside the wooden mass: the decay due to the thermal decomposition process shows continuously new "defects" of the timber elements and consequently it is more than likely that the composite structure  $S_3$  (with lower value of the initial static efficiency) exhibits the smallest value of the ratio  $q_u/q_{sl}$ .

Timber-based composite structures		$q_{sl}$ ( $\text{kN}\cdot\text{m}^{-2}$ )	$q_u$ ( $\text{kN}\cdot\text{m}^{-2}$ )	$q_u/q_{sl}$
S1	Concrete slab (glued steel connectors)	13.01	33.33	2.56
S2	Laminated wood panel slab (glued steel connectors)	11.93	27.66	2.32
S3	Laminated wood panel slab (screw connectors)	8.71	15.13	1.74
S4	Plywood boards slab (glued steel connectors)	11.96	26.54	2.22
Beam <sup>(1)</sup>	Single timber beam	3.96	10.50	2.65

Table II - The static performance of the residual timber composite structures after fire.

Worthy of another mention is the problem related to the determination of the ultimate limit state of glued connections due to heat, when the glue is sensitive to high temperatures. This problem is quite easily resolved at the design stage: all that is necessary is to guarantee an adequate protection for the glue beneath the charred layer. The thickness of wood required for the glue used here (with a "softening" temperature of  $\approx 80^\circ\text{C}$ ) has given a value ranging from 20 to 25 mm.

#### 4. Concluding Remarks

Timber-based composite structures are generally very sensitive to the bending and axial stiffness of the component elements as well as to the stiffness (due to shear force) of the connection. Consequently, if the structure is exposed to fire, it is essential to have a sufficiently accurate knowledge of the stiffness variations that the single elements are subject to, in order to set prediction models for the composite structure's behaviour and, especially, to determine its resistance to fire. The physical tests performed up till now reveal that actual standard's decay models are not adequate in order to accurately define the bending stiffness of timber elements during fire and, therefore, the behaviour of the whole composite structure.

#### Acknowledgements

The authors would like to thank the M.U.R.S.T. (the Italian Ministry for the University and the Scientific Research) for the partial financial support to the research, still in progress.

#### References

- [1] ENV 1995-1-2; Eurocode 5: Design of Timber Structures - Part 1-2: General Rules- Structural Fire Design; European Committee for Standardisation, 1994.
- [2] U.N.I.-C.N.VV.F. 9504; Analytical Fire Resistance Assessment of Timber Structural Elements; 1989.
- [3] BALLERINI, M.; CONT, S.; PIAZZA, M.; ZANON, P.; Some Aspects on the Behaviour of Timber-Based Mixed Structures Exposed to Fire; PTEC '94, Gold Coast, Australia, 1994.
- [4] NATTERER, J.; HERZOG, T.; VOLZ, M.; Holzbau Atlas Zwei; Institut für Internationale Architektur-Dokumentation GmbH, München, 1991.
- [5] PIAZZA, M.; TURRINI, G.; Il comportamento statico della struttura mista legno-calcestruzzo; Recuperare n. 6, 1983.
- [6] PIAZZA, M.; TURRINI, G.; The Influence of Connector Flexibility on the Behaviour of Composite Beams; Costruzioni Metalliche, n.6, 1986.
- [7] PIAZZA, M.; Restoration of Timber Floors via a Composite Timber-Timber Solution; Workshop RILEM "Timber: A structural Material from the Past to the Future", Trento, 1994.

## Global Fire Safety Concept for Buildings

**Louis-Guy CAJOT**  
 Civil Engineer  
 Profil ARBED Research  
 Esch/Alzette, Luxembourg

**Jean-Baptiste SCHLEICH**  
 Civil Engineer  
 Profil ARBED Research  
 Esch/Alzette, Luxembourg

### Summary

In order to establish the basis for realistic and credible assumptions to be used in the fire situation for thermal actions, active measures and structural response, a new European Research financed by ECSC entitled "Competitive Steel Buildings through Natural Fire Safety Concept", started in 1994 [1]. It is being performed by 10 partners out of 11 European countries and is co-ordinated by PROFILARBED-Research. This paper describes the state of the art of the research

### Introduction

Fire Engineering design is a recent discipline which is progressing constantly and dynamically. The fire was seriously taken into account in the construction only at the end of the sixties after dramatic fires which are still in all minds.

At the beginning, the only possibility to determine the fire resistance of a building element was to perform a test in a laboratory. The element was subjected in a furnace to an increase of gas temperature according to the normalised ISO curve with 821°C after 30 minutes, 925°C after 60 minutes and 1029°C after 120 minutes. Unfortunately this standard temperature-time curve involves an ever increasing air temperature inside the considered compartment, even when later on all consumable materials have been destroyed. In fact, after a given time, depending on the fire load and the ventilation conditions, the air temperature will necessarily decrease. The application of this unrealistic ISO Standard leads necessary to very different requirements from one country to another. For example, open car parks may be built with unprotected steel on one side of the Rhine and need 90 minutes of ISO fire resistance on the other side ! Big discrepancies exist in the fire resistance requirements of the European countries for all types of buildings ranging from industrial halls to high rise buildings.

In order to establish the basis for realistic and credible assumptions to be used in the fire situation for thermal actions, active measures and structural response, a new European Research [1] entitled "Competitive Steel Buildings through Natural Fire Safety Concept", started in 1994. The aim is to develop a **Global Fire Safety Concept** which deals with the Safety for Occupants, Fire-fighters and Structures. That's why we have to perform a structural analysis of the whole structure in the fire situation, consider a realistic i.e. accidental combination of loads, adopt for the fire simulation a natural fire curve depending on the fire load and the ventilation conditions. In a second step, the active fire fighting measures such as detection systems, alarms, sprinklers, ... are taken into account and their influence on the probabilistic reduction of the fire event and consequently on the improvement of the building Safety, is quantified.

The aim of this paper is to describe the state of the Art of this European research which implies 4 Working Groups (see figure 1).

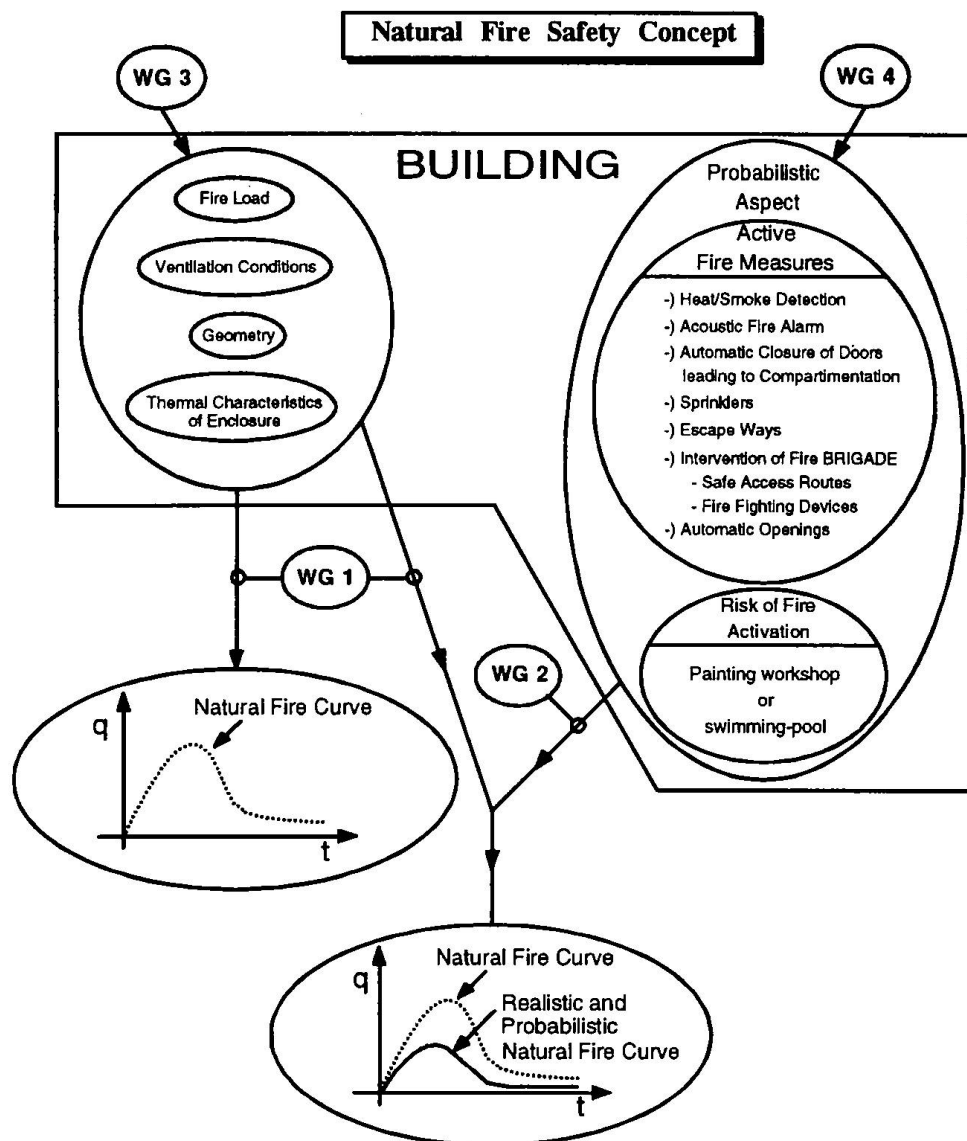


Figure 1: General guidelines of the research "Natural Fire Safety Concept "

## 1. Working Group 1: Natural Fire Models

The goal is to provide some ways to replace the ISO curve which has 3 main defects:

- The ISO curve has to be considered for the whole compartment even if this compartment is huge
- The ISO curve never goes down and implies an air temperature increasing to the moon!
- There is only one ISO curve for all the types of building, whatever the fire load or the ventilation conditions.

In order to answer to the first critics, a procedure has been defined to check whether the fire remains a localised fire or spreads and becomes a fully engulfed compartment fire. In case of localised fire a method has been developed to calculate the 4-dimensional temperature field  $\theta(x,y,z,t)$ . The two other defects are already dealt with in the annex B of ENV 1991-2-2 [2] which provides a first alternative to the ISO-curve and considers the fire load, the openings and the thermal characteristics of the walls (see figure 2).

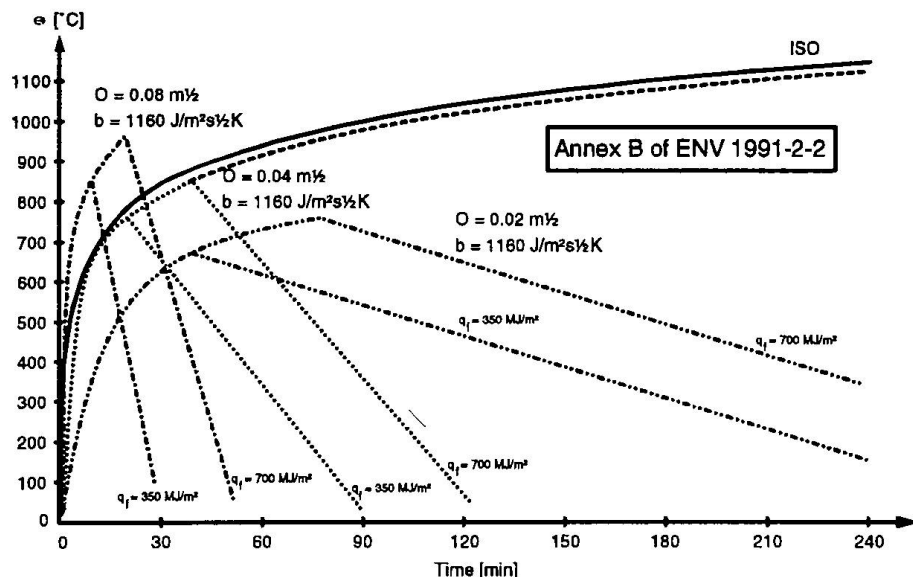


Figure 2: Annex b of ENV 1991-1

The Working Group 1 has improved this annex B in order to consider the fuel bed controlled regime; they are developing a programme One Zone model called OZONE which contains, in addition to the available One Zone programs, a combustion model to define itself the burning regime (fuel bed or ventilation controlled) and a sophisticated wall model which is really included in the air temperature calculation. Moreover they are collecting natural fire tests in order to create a database which enables us to check the models. Concerning the localised fire they have analysed the different air entrainment models which have a large influence on the temperature and the height of the smoke zone.

## 2. Working Group 3: Fire characteristics

To be able to use these calculation tools, it is necessary to know the fire characteristics such as the fire load, the Rate of Heat Release, the ventilation conditions, the thermal inertia of the compartment walls, the parameters defining the fire spread, the conditions leading to a flash-over, the amount of smoke entrained by the fire and the model of combustion that defines the oxygen needed for combustion, that reduces the peak of the Rate of Heat Release and increases the fire duration in case of lack of oxygen. It is the task of Working Group 3 to provide all these data.

## 3. Working Group 2: Probabilistic aspects

The probability that a fire breaks out in a swimming-pool is obviously much lower than in a painting workshop. Moreover the probability that this starting fire spreads and leads to a fully engulfed compartment depends of course of the active fire fighting measures such as the sprinklers which may extinguish automatically the fire, the firemen or the automatic fire detection (by smoke or heat) and the automatic transmission of the alarm to the firemen which allows a rapid fire brigade intervention.

Concerning the influence of the sprinklers, some surveys, some tests and numerical simulations attest that there is no risk for the stability of the structure if the sprinkler system has been well designed and works when a fire breaks out. The influence of the sprinklers on the structure behaviour is thus only a question of reliability. Will the sprinklers work when necessary ?

In order to quantify the influence of the active measures, the approach described in ENV 1991-1 has been used. The Eurocode 1 Part 1-1 concerning the actions and the resistance values is based on a probabilistic concept that has lead to safety coefficients  $\gamma$ , so that this concept can be applied in practice. The safety factors  $\gamma$  for the actions and the material properties has been deduced by a semi-probabilistic approach (Annex A of ENV 1991-1) which assumes implicitly a target failure probability of  $7\text{E-}5$  per working life of the building, which is equivalent to a safety factor  $\beta$  of 3,8 :  $p_f$  (failure probability)  $\leq p_t$  (target probability) (1).

In case of fire, the main action is the fire which can be quantified by the fire load expressed in kg of wood or in MJ. However, this fire load becomes a real action for the structure only when there is a fire. The fire load influences really the structure only with a certain probability  $p_{acc}$ ,  $p_{acc}$  being the product of  $p_1$  (probability that a fire starts) and  $p_2$  (probability that this starting fire turns to a flash-over or a fully engulfed compartment).

In case of fire which is considered as an accidental action the equation (1) becomes  $p_f$  (failure probability in case of fire) \*  $p_{acc}$  (probability of fire)  $\leq p_t$  (target probability). In that way the  $\beta$  is no more equal to the constant value 3,8 but depends of the probability that there is a fully engulfed fire compartment during the building life. Indeed the safety index  $\beta$  has to be determined by using  $p_{t,fi}$  which is equal to  $(p_t / p_{acc})$  (see figure 3) and enables us to determine the corresponding safety factor  $\gamma_i$  for the static loads, the material properties and the fire load.

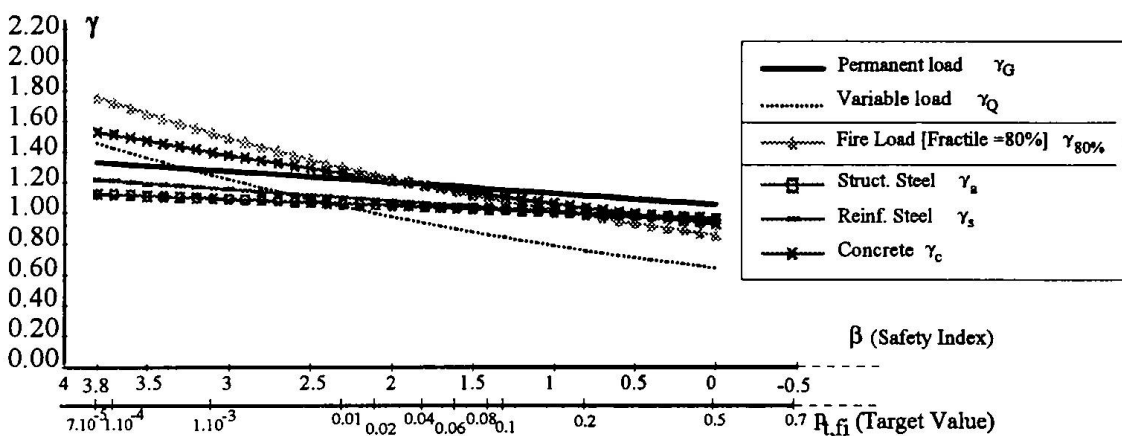


Figure 3: Global safety factor  $\gamma$  on the static loads, on the materials properties and on the fire loads

However this global procedure implies the calculation of the fire probability for each case. That's why we have developed a simplified approach which consists of splitting the safety factor  $\gamma_{fire load}$  into 3 coefficients  $\gamma_{q1}$  to consider the compartment size,  $\gamma_{q2}$  to consider the risk of fire activation and  $\gamma_{ni}$  to take into account the influence of the active measures.

According to the background of the DIN 18230 [3], the probability to have a fully engulfed compartment per  $\text{m}^2$  per year in the schools, hotels, or offices is equal to  $5 \cdot 10^{-7}$ .

By multiplying by 50, we obtain the probability for the complete life of the building estimated to 50 years: Probability of a compartment fully engulfed by the fire :  $p_1 p_2 = 5 \cdot 10^{-7} \cdot 50 = 25 \cdot 10^{-6}$ . Let us assume in a first step a compartment area  $A_f = 25\text{m}^2$ .

With these values, the probability  $p_{acc}$  of a fully engulfed compartment is :  $p_{acc} = p_1 p_2 A_f = 6,25 \cdot 10^{-4}$

The target value of the failure in case of fire  $p_{t,fi}$  becomes then :  $p_{t,fi} = \frac{p_t}{p_{acc}} = \frac{7 \cdot 10^{-5}}{6,25 \cdot 10^{-4}} = 0,112$  and

the corresponding safety index  $\beta_{fi}$  is equal to 1,2. This factor  $\beta$  of 1,2 implies a safety factor  $\gamma$  of 1,0 in case of 80 % fractile for the characteristic fire load (see figure 3).

In the same way, we can obtain other safety coefficients  $\gamma$  for other compartment areas  $A_f$  as follows :

$A_f [m^2]$	$p_{acc}$	$P_t / p_{acc}$	$\beta$	$\gamma_{q1}$
25	$6,25 \cdot 10^{-4}$	0,11200	1,22	1,0
250	$6,25 \cdot 10^{-3}$	0,01120	2,28	1,25
2500	$6,25 \cdot 10^{-2}$	0,00112	3,03	1,5
5000	$12,5 \cdot 10^{-2}$	0,00056	3,26	1,6
10000	$25,10^{-2}$	0,00028	3,45	1,65

The previous calculation is based on a probability of fire  $p_1 p_2$  of  $5 \cdot 10^{-7}$  per year and  $m^2$  corresponding to schools, offices or hotels. It is obvious that the risk is much higher for a fireworks industry and lower for a museum with Grecian statues.

For a building of  $2500 m^2$ , the safety coefficient  $\gamma$  is equal to 1,5. What happens if the probability of having a fire is reduced by 10 ? From the figure 3 it can be deduced that the safety coefficient  $\gamma$  is reduced by a factor 0,85. Moreover, this factor 0,85 is rather constant if we make a variation on  $\beta$ . In this way, the buildings can be classified according to the danger of fire activation. For each class, it is possible to deduce an additional safety coefficient  $\gamma_{q2}$  according to the following table :

Type of building destination	Danger of fire activation	$(p_1 p_2)$	$\gamma_{q2} = \frac{\gamma}{\gamma_{normal}}$
		$(p_1 p_2)_{normal}$	
Museum, Art gallery	low	$10^{-1}$	0,85
Hotel, School, Office	normal	1	1
Engine Fabrication	average	10	1,2
Painting Workshop, Chemistry Laboratory	high	100	1,4
Painting Fabrication, Fireworks Industry	higher	1000	1,6

In the same way, it is possible to quantify the influence of active fire fighting measures. Each active measure reduces the probability that a starting fire turns to a flash-over or a fully engulfment of the compartment.

Official Document	$\gamma_{ni}$ Function of Active Fire Safety Measures										$\gamma_n^{\min} = \gamma_{n1} \dots \gamma_{n10}$	
	Automatic Fire Suppression		Automatic Fire Detection			Manual Fire Suppression						
	Automatic Water Extinguishing System	Independent Water Supplies	Automatic fire Detection & Alarm by Heat	Automatic Alarm Transmission to Fire Brigade	Work Fire Brigade	Off Site Fire Brigade	Safe Access Routes	Normal Fire Fighting Devices	Smoke Exhaust System			
Title	Date of publication	$\gamma_{n1}$	$\gamma_{n2}$	$\gamma_{n3}$	$\gamma_{n4}$	$\gamma_{n5}$	$\gamma_{n6}$	$\gamma_{n7}$	$\gamma_{n8}$	$\gamma_{n9}$	$\gamma_{n10}$	
SIA 81 [5]	1984	0,50 0,59			0,83 or 0,69	0,83	$\gamma_{n6}, \gamma_{n7} = 0,53$		0,67 or 0,63	1,0 1,39*	0,85	0,13 0,49
ANPI [4]	1988	0,58	0,86   0,65	0,82   0,68	included in	0,50	0,68			1,0 1,36*		0,07 0,48
DIN V 18230-1 [3]	1987/95	0,60			0,90		0,60					0,32 0,54
ENV 1991-2-2 [2]	1995	0,60										0,60
NFSC PROPOSAL [1]	1997	0,70	1,0   0,95   0,9	0,90	0,80	0,90	0,70	0,85	$0,9 \text{ or } 1$ 1,5*	1,0 1,4*	1,0 1,5*	0,22 0,63

Figure 4: Differentiation factor  $\gamma_{ni}$  accounting for various active fire safety measures.

Therefore, for each active measure it is possible to deduce a coefficient  $\gamma_n$  smaller than 1 to take into account the sprinklers, the firemen, the detection measures and higher than 1 to consider that some elementary measures, as for example the extinguishers on each storey, are not fulfilled. It is

interesting to compare the coefficients  $\gamma_{ni}$  deduced from probabilistic considerations with other coefficients resulting from other methods which are based on empirical backgrounds (see figure 4).

#### 4. Working Group 3: Statistics

The Working Group 4 is collecting statistics about real fires and about failure of active measures (A.M.). Its objectives is to deduce from these real statistics the probabilities needed for the probabilistic approach developed by the Working Group 2.

Type of Occupancies	Fire Probability	$P_1 P_2$	Automatic fire suppression	Failure Probability of the active measure	
				without A.M. $P_{acc}$	With A.M. $P_{acc}$
Museum, Artgallery	small	$25 \cdot 10^{-7}$	Sprinkler (S)	0,01	100
Residence, Hotel, Office	normal	$25 \cdot 10^{-6}$	S + 1 Independent Water Supply	$0,01 \cdot 0,5$	$100 \cdot 2$
Manufactory of machinery	mean	$25 \cdot 10^{-5}$	S + 2 Independent Water Supply	$0,01 \cdot 0,25$	$100 \cdot 4$
Painting Workshop	high	$25 \cdot 10^{-4}$	Work Fire Brigade (WFB)	0,01	100
Manufactory of paints, Manufactory of fireworks	very high	$25 \cdot 10^{-3}$	Standard Fire Brigade (SFB)	0,1	10
			SFB + Automatic fire detection by heat	$0,1 \cdot 0,25$	$10 \cdot 4$
			SFB + Automatic fire detection by smoke (ADS)	$0,1 \cdot 0,0625$	$10 \cdot 16$
			SFB + ADS + Automatic Alarm Transmission to Fire Brigade	$0,1 \cdot 0,0625 \cdot 0,25$	$10 \cdot 16 \cdot 4$

Figure 5: Probabilities deduced from statistics.

#### 5. Conclusion

The coefficients  $\gamma_{ni}$  et  $\gamma_{qi}$  enable us to quantify the risk of fire and the influence of the active fire fighting measures, to deduce a design fire load which will be used to calculate a fire curve and a resistance time  $t_{fi,d}^{nat}$ . This resistance time will have to be compared with the required time  $t_{fi,req}$  which depends on the evacuation time and the consequences of the failure of the structure. This approach is quite easy to be used and at the same time is based on a safe scientific background issued from the ECSC research [1].

This Global Fire Safety Concept has been applied in practice to the new ARBED Office Building in Esch/Alzette. This allowed to use a steel frame without insulating material or any intumescent paint and to have it fully visible inside the atrium areas.

#### 6. References

- [1] SCHLEICH J.B.; Competitive steel buildings through natural fire safety concept. ECSC Research 7210-SA/522 etc., B-D-E-F-I-L-NL-UK & ECCS, 1994-98.
- [2] CEN; ENV 1991-2-2, Eurocode 1 - Basis of design and actions on structures, Part 2.2 - Actions on structures exposed to fire. CEN Central Secretariat, Brussels, DAV 09.02.1995.
- [3] DIN; Baulicher Brandschutz im Industriebau - Teil 1: Rechnerisch erforderliche Feuerwiderstandsdauer. DIN V18230-1, Beuth Verlag GmbH, Berlin, 1995.
- [4] ANPI; Evaluation des risques. Association Nationale pour la Protection contre l'Incendie, Ottignies, 1988.
- [5] SIA; Brandrisikobewertung, Berechnungsverfahren. Dokumentation SIA 81, Zürich, 1984.